Carbonates in the Critical Zone

Matthew David Covington[1,2], J B Martin[3], L E Toran[4], J L Macalady[5], N Sekhon[6], P.L. Sullivan[7], Á A García[8], J B Heffernan[9], and W D Graham[3,10,11,12]

[1]Department of Geosciences, University of Arkansas
[2]ZRC SAZU, Karst Research Institute, Slovenia
[3]Department of Geological Sciences, University of Florida
[4]Department of Earth and Environmental Science, Temple University
[5]Department of Geosciences, Pennsylvania State University
[6]Department of Earth, Environmental and Planetary Science
[7]College of Earth, Ocean, and Atmospheric Science, Oregon State University
[8]Department of Geology and Environmental Science, James Madison University
[9]Nicholas School of the Environment, Duke University
[10]Geology and Environmental Science, Nicholas School of the Environment, James Madison University
[11]Duke University
[12]University of Florida

December 27, 2022

Abstract

Earth's Critical Zone (CZ), the near-surface layer where rock is weathered and landscapes co-evolve with life, is profoundly influenced by the type of underlying bedrock. Previous studies employing the CZ framework have focused primarily on landscapes dominated by silicate rocks. However, carbonate rocks crop out on approximately 15% of Earth's ice-free continental surface and provide important water resources and ecosystem services to ~1.2 billion people. Unlike silicates, carbonate minerals weather congruently and have high solubilities and rapid dissolution kinetics, enabling the development of large, interconnected pore spaces and preferential flow paths that restructure the CZ. Here we review the state of knowledge of the carbonate CZ, exploring parameters that produce contrasts in the CZ in different carbonate settings and identifying important open questions about carbonate CZ processes. We introduce the concept of a carbonate-silicate CZ spectrum and examine whether current conceptual models of the CZ, such as the conveyor model, can be applied to carbonate landscapes. We argue that, to advance beyond site-specific understanding and develop a more general conceptual framework for the role of carbonates in the CZ, we need integrative studies spanning both the carbonate-silicate spectrum and a range of carbonate settings.

1 # Carbonates in the Critical Zone

2 **M. D. Covington[1,2], J. B. Martin[3], L. E. Toran[4], J. L. Macalady[5], N. Sekhon [6,7], P. L.**
3 **Sullivan[8], Á. A. García, Jr.[9], J. B. Heffernan[10], and W. D. Graham[11]**

4 [1]Department of Geosciences, University of Arkansas, Fayetteville, AR, USA. [2]ZRC SAZU,
5 Karst Research Institute, Slovenia. [3]Department of Geological Sciences, University of Florida,
6 Gainesville, FL, USA. [4]Department of Earth and Environmental Science, Temple University,
7 Philadelphia, PA, USA [5]Department of Geosciences, Pennsylvania State University, State
8 College, PA, USA [6]Department of Earth, Environmental and Planetary Science, Brown
9 University, Providence 02908, Rhode Island, United States [7]Institute at Brown for Environment
10 and Society, Brown University, Providence 02908, Rhode Island, United States [8]College of
11 Earth, Ocean, and Atmospheric Science, Oregon State University, OR, USA [9]Department of
12 Geology and Environmental Science, James Madison University, Harrisonburg, VA, USA
13 [10]Nicholas School of the Environment, Duke University, Durham, NC [11]University of Florida
14 Water Institute, Gainesville, FL, USA

15 Corresponding author: Matthew D. Covington (mcoving@uark.edu)

16 **Key Points:**

17 • A holistic understanding of Earth's critical zone requires integrative studies spanning the
18 spectrum of carbonate and silicate landscapes.

19 • Porosity developed by congruent dissolution of carbonates decouples hillslopes from
20 stream channels, altering topographic equilibrium.

21 • Shifts in carbonate critical zone structure from changing ecology, land use, and climate
22 may be rapid because of fast dissolution kinetics.

Abstract

Earth's Critical Zone (CZ), the near-surface layer where rock is weathered and landscapes co-evolve with life, is profoundly influenced by the type of underlying bedrock. Previous studies employing the CZ framework have focused primarily on landscapes dominated by silicate rocks. However, carbonate rocks crop out on approximately 15% of Earth's ice-free continental surface and provide important water resources and ecosystem services to ~1.2 billion people. Unlike silicates, carbonate minerals weather congruently and have high solubilities and rapid dissolution kinetics, enabling the development of large, interconnected pore spaces and preferential flow paths that restructure the CZ. Here we review the state of knowledge of the carbonate CZ, exploring parameters that produce contrasts in the CZ in different carbonate settings and identifying important open questions about carbonate CZ processes. We introduce the concept of a carbonate-silicate CZ spectrum and examine whether current conceptual models of the CZ, such as the conveyor model, can be applied to carbonate landscapes. We argue that, to advance beyond site-specific understanding and develop a more general conceptual framework for the role of carbonates in the CZ, we need integrative studies spanning both the carbonate-silicate spectrum and a range of carbonate settings.

Plain Language Summary

Carbonate landscapes, which cover ~15% of Earth's land surface and provide critical water resources and other services to ~1.2 billion people, require focused studies to understand how life and rocks interact. Most integrated studies of this "critical zone" focus on landscapes underlain by silicate minerals instead of considering the full spectrum of the minerals that make up bedrock. Weathering extends to greater depths in carbonate landscapes compared with silicate landscapes, leading to the development of interconnected subsurface flow systems that transport both water and sediments. As a result, the flow of water and the movement of materials left behind by weathering rock may be disconnected from streams, unlike in silicate landscapes. Furthermore, responses of the carbonate critical zone to changes in land use and climate may be rapid because carbonate rocks dissolve faster than silicate rocks. Integrative studies of silicate, carbonate, and mixed silicate-carbonate landscapes will be required to construct a holistic understanding of Earth's critical zone.

1 Introduction

The objectives of this paper are to review the state of knowledge of critical zone (CZ) processes in carbonate terrains, to advance a framework that serves to bridge the spectrum between carbonate and silicate CZ endmembers (Martin et al., 2021), and to identify key knowledge gaps in our understanding of the carbonate CZ. Earth's CZ is the region where landscapes co-evolve with life and is loosely defined as the zone from the base of continental crust weathering to the top of the vegetation canopy (National Research Council, 2001). The CZ develops through interactions among geological, hydrological, chemical, biological, and climate processes. Understanding the scope of, and linkages between, these interactions requires interdisciplinary collaborations, to unravel how the CZ functions and responds to environmental perturbations, including human impacts on climate, land use, and global elemental cycling. The U.S. scientific community has engaged in focused research on Earth's CZ through the development of place-based Critical Zone Observatories (CZOs) (Brantley et al., 2017b), leading to the more recent development of theme-based Critical Zone Networks (CZNs). The CZO/CZN sites span a variety of geological and climate settings across the U.S. However, the CZ

67 framework is limited by a CZO/CZN focus on landscapes underlain by silicate rocks (Martin et
68 al., 2021). Globally, scientists are beginning to establish CZ observatories on carbonate rocks
69 (Gaillardet et al., 2018; Jourde et al., 2018; Quine et al., 2017), but carbonates remain
70 underrepresented among the studies employing the CZ framework. Although prior and ongoing
71 studies provide useful information about localized carbonate terrains, more synthesis and a better
72 predictive understanding of the carbonate CZ will require integrative studies of multiple
73 carbonate settings with varied characteristics. Such a synthesis could also improve fundamental
74 understanding of the silicate dominated CZ, as weathering of carbonates is also important within
75 predominantly silicate settings (e.g. Brantley et al., 2013), and many landscapes fall on a
76 continuum between the carbonate and silicate endmembers.

77   A focus on terrains where the CZ is dominated by carbonate minerals is justified by their
78 common occurrence, their influence on society and its resource base, and their role in the human
79 experience and human culture. Approximately 15% of Earth's ice-free continental surface
80 contains carbonate rock (Figure 1), and approximately 1.2 billion people, 16% of the Earth's
81 population, reside on carbonate rock (Goldscheider et al., 2020). Landscapes developed by the
82 dissolution of carbonate terrains, also known as karst, often appear as a central theme in cultural
83 development among long-term communities (groups that have been residing in the same
84 locations for generations) around the world. Karst landforms and features have influenced
85 Indigenous creation stories, place-naming (toponymy), culturally based geological interpretation,
86 and local language adaptation in the Greater Antilles part of the Caribbean (Alvarez Nazario
87 1972; Dominguez-Cristobal 1989, 1992, 2007; Garcia et al., 2020; Pané 1999), as well as a form
88 of wealth building in central Europe that goes back to the 17th century (Zorn et al., 2009). In
89 addition, the conservation of karst features has become a global priority because they commonly
90 link geological, ecological, cultural, archeological, and touristic resources (Williams, 2008a).
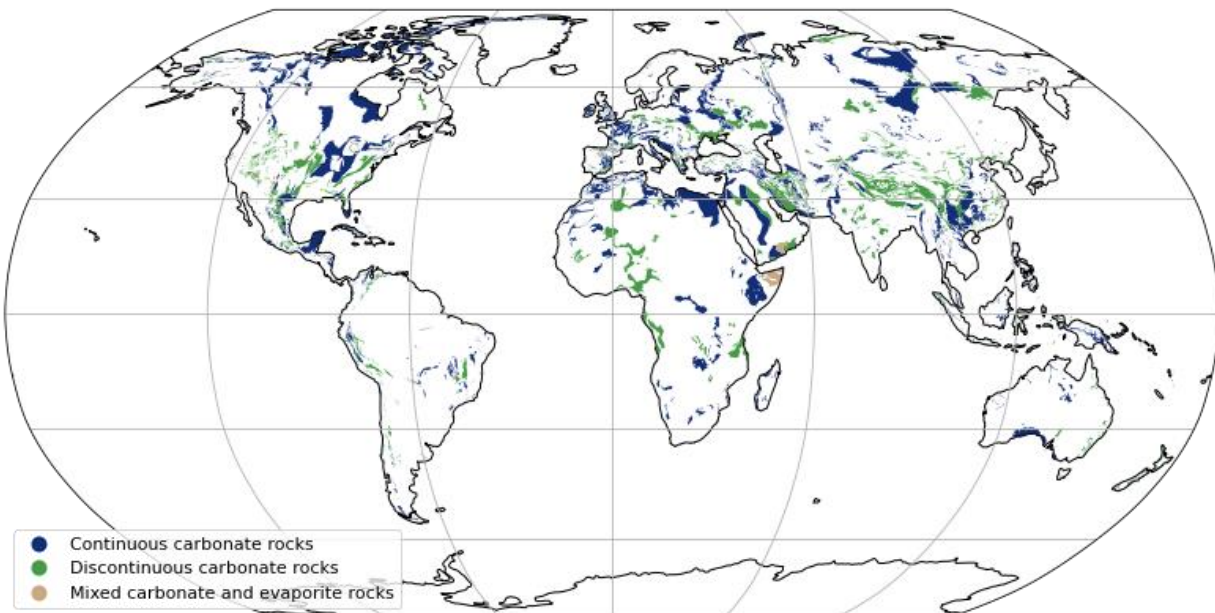

91
92 **Figure 1.** Carbonate exposures across the surface of Earth using data from the World Karst
93 Aquifer Map (data from Goldscheider et al., 2020). Areas with more than 65% carbonate rocks
94 are mapped as continuous, whereas areas with between 15% and 65% carbonates are mapped
95 as discontinuous. Areas with greater than 15% of both carbonates and evaporites are mapped
96 as mixed.

97

98   Carbonate terrains provide a wide range of societal and ecological services and present a
99   variety of unique hazards. Given the favorable conditions for groundwater extraction from
100 carbonates, and the ubiquity of springs within carbonate terrains, aquifers that develop in
101 carbonate rocks are a crucial component of the global water supply (Ford and Williams, 2007;
102 Worthington et al., 2016). Hazards unique to carbonate terrains, such as sinkholes and
103 groundwater flooding, cause significant economic losses in densely populated areas (De Waele
104 et al., 2011). Carbonate aquifers are particularly susceptible to contamination due to rapid travel
105 times and limited natural remediation within large pores and conduits (White et al., 2016).
106 Carbonate rocks are the largest global reservoir of carbon and have a potentially important, yet
107 uncertain, role in the global carbon cycle over timescales relevant for rapid climate change
108 (Baldini et al., 2018; Gaillardet et al., 2019; Martin, 2017). The raw materials for cement
109 manufacturing are produced from carbonate rocks by calcination converting $CaCO_3$ to CaO plus
110 CO_2, thereby producing 13% of the world's industrial CO_2 emissions (Fischedick et al., 2014).
111 Carbonate minerals provide important pH buffering capacity within aquatic systems.
112 Subterranean habitats within carbonate terrains host a wide variety of endemic species, many of
113 which are threatened or endangered (Culver and Pipan, 2013). The carbonate CZ provides
114 unique opportunities for study because of the ability for humans to access it at depth within
115 caves. Interpretation of speleothem records within caves, which are an important source of
116 paleoclimate information, requires substantial understanding of carbonate CZ processes, as
117 signals recorded in speleothems are first filtered through the upper portion of the CZ (Fairchild et
118 al., 2006; Fohlmeister et al., 2020). Consequently, studies of cave drip water have provided
119 substantial insight into carbonate CZ dynamics (e.g., Tobin et al., 2021; Treble et al., 2022).
120 Because of rapid mineral dissolution processes within, and subsurface fluxes through, the
121 carbonate CZ, carbonate CZ systems may act as a bellwether for CZ responses to climatic and
122 human perturbations (Sullivan et al., 2017). Furthermore, carbonate minerals often make up an
123 important component of other sedimentary rocks (Hartmann and Moosdorf, 2012), and their
124 distinct weathering characteristics can control weathering of non-carbonate minerals. The many
125 impacts of carbonate minerals underscore the need for focused studies of carbonates in Earth's
126 CZ.

127 2. Exploring the carbonate endmember

128   We begin with a review of current understanding of carbonate CZ processes. Within
129 carbonate terrains, geological, hydrological, biological, geochemical, and climate variables
130 produce a broad array of carbonate CZ characteristics. Here, we explore the range of parameters
131 that create important differences in the carbonate CZ in different settings.

132   2.1 The importance of porosity distributions

133   Where the CZ occurs in nearly pure carbonate terrains, it is often transformed through
134 congruent dissolution into karst, a landscape formed by dissolution of rock that develops
135 underground drainage networks (Ford and Williams, 2007). Most karst landscapes form in
136 carbonate bedrock, because of its common occurrence, although they also develop in evaporites
137 (Klimchouk et al., 1996; Frumkin, 2013) and occasionally, in less soluble rocks (e.g., Wray and
138 Sauro, 2017). Dissolution integrates subsurface flow networks as water penetrates along
139 heterogeneities in the rock until solutionally enlarged flow paths link input to outpoint points
140 (Dreybrodt, 1990; Ford et al., 2000; Palmer, 1991). Such integrated flow paths, or karst conduits,
141 are characterized by elevated permeability and exhibit rapid and turbulent flow that transports

142   large quantities of solutes and gases between the surface and subsurface. High flow rates also
143   allow the conduits to transport sediment through the subsurface (Cooper and Covington, 2020;
144   Farrant and Smart, 2011; Herman et al., 2012). Once the capacity of the subsurface conduit
145   network is sufficient to carry available surface runoff and sediment, closed basins develop on the
146   land surface that route water and sediment into the subsurface. Conduit systems exit at springs,
147   which frequently develop near the local hydrological base level. Together, these processes lead
148   to the dolines, caves, and springs that characterize karst landscapes.

149   Karst aquifers are commonly conceptualized as a triple-porosity system, in which
150   porosity is divided into a matrix component, a fracture component, and a conduit component
151   (Quinlan et al., 1996; White, 2002; Worthington, 1999). The matrix component represents the
152   primary porosity of the bedrock. The fracture component represents secondary porosity as a
153   result of fractures and bedding partings. The conduit component represents dissolutionally
154   enlarged flow paths that have increased connectivity as a result of positive feedback between
155   dissolution and flow focusing (Worthington et al., 2016). While the dividing line between
156   conduits and fractures is somewhat arbitrary, often the conduits are defined as the flow paths that
157   carry turbulent flow (White, 2002). The three porosity components differ in their ability to store
158   and transmit water. Primary porosity provides much more storage than the conduit network,
159   because of its large total volume, whereas conduits transmit the most water, because of their high
160   permeability (Worthington, 1999). These different hydrologic characteristics create a strong
161   scale-dependent hydraulic conductivity in karst aquifers. Hydraulic conductivity over short
162   distances is controlled by the primary porosity and is thus relatively low. Hydraulic conductivity
163   increases over intermediate distances as fractures become important and is greatest at aquifer
164   scales where flow through conduits dominates (Halihan et al., 2000; Király, 1975; Worthington,
165   2009). In general, heterogenous media exhibit an increase of hydraulic conductivity with
166   measurement scale, up to some cutoff scale where the medium is well-represented by an
167   equivalent porous medium (Schulze-Makuch et al., 1999). However, the range of variation in
168   hydraulic conductivity is largest in karstified media, as karst exhibits the largest cutoff scale
169   (Schulze-Makuch et al., 1999), with individual aquifers having measured values of hydraulic
170   conductivity ranging over more than eight orders of magnitude (Worthington, 2009).

171   The primary porosity within a carbonate rock is a function of its diagenetic history and
172   whether the rock has undergone burial diagenesis, which reduces primary porosity. The terms
173   eogenetic karst and telogenetic karst are used to distinguish karst that is developed within
174   relatively young carbonates that have primarily undergone meteoric (eogenetic) diagenesis from
175   karst developed in older carbonates that have experienced burial diagenesis (telogenetic) and re-
176   exposure to the surface via erosion (Vacher and Mylroie, 2002; Choquette and Pray, 1970).
177   Integrated karst flow networks develop most easily in rocks with relatively low primary porosity
178   and relatively high fracture porosity (Palmer, 1991; White, 1969; Worthington, 2014). Such
179   conditions focus flow through higher permeability fractures, increasing flow velocities and the
180   depth to which undersaturated water can penetrate the rock, ultimately leading to breakthrough
181   of dissolutionally enlarged pathways that connect inlets to outlets (Dreybrodt, 1990). Positive
182   feedback further focuses the flow, whereby the most efficient flow paths receive the most flow
183   and therefore grow most rapidly, diverting even more flow into these pathways and further
184   accelerating their growth (Ewers, 1982; Palmer, 1991; Siemers and Dreybrodt, 1998). The
185   largest developing flow paths create troughs in the potentiometric surface, such that other
186   competing pathways are drawn toward them, frequently producing a dendritic pattern like that
187   found in surface stream networks. The overall conduit network geometry is strongly influenced

188 by the nature of recharge to the aquifer and the locations of recharge and outlet points (Figure 2)
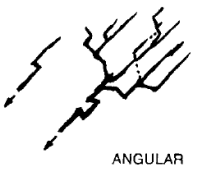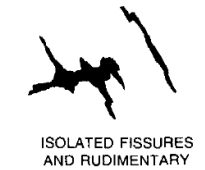189 (Palmer, 1991).

190
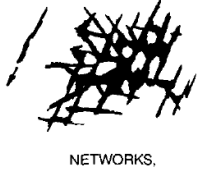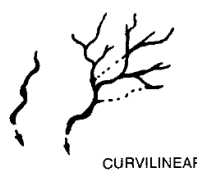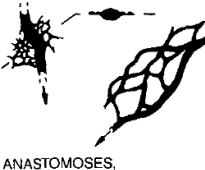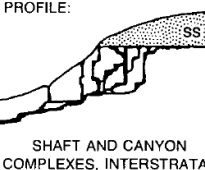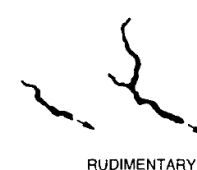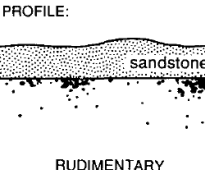
TYPE OF RECHARGE					
	VIA KARST DEPRESSIONS		**DIFFUSE**		**HYPOGENIC**
	SINKHOLES (LIMITED DISCHARGE FLUCTUATION)	SINKING STREAMS (GREAT DISCHARGE FLUCTUATION)	THROUGH SANDSTONE	INTO POROUS SOLUBLE ROCK	DISSOLUTION BY ACIDS OF DEEP-SEATED SOURCE OR BY COOLING OF THERMAL WATER
	BRANCHWORKS (USUALLY SEVERAL LEVELS) & SINGLE PASSAGES	SINGLE PASSAGES AND CRUDE BRANCHWORKS, USUALLY WITH THE FOLLOWING FEATURES SUPERIMPOSED:	MOST CAVES ENLARGED FURTHER BY RECHARGE FROM OTHER SOURCES	MOST CAVES FORMED BY MIXING AT DEPTH	

DOMINANT TYPE OF POROSITY

FRACTURES	ANGULAR PASSAGES	FISSURES, IRREGULAR NETWORKS	FISSURES, NETWORKS	ISOLATED FISSURES AND RUDIMENTARY NETWORKS	NETWORKS, SINGLE PASSAGES, FISSURES
BEDDING PARTINGS	CURVILINEAR PASSAGES	ANASTOMOSES, ANASTOMOTIC MAZES	PROFILE: SS / SHAFT AND CANYON COMPLEXES, INTERSTRATAL SOLUTION	SPONGEWORK	RAMIFORM CAVES, RARE SINGLE-PASSAGE AND ANASTOMOTIC CAVES
INTERGRANULAR	RUDIMENTARY BRANCHWORKS	SPONGEWORK	PROFILE: sandstone / RUDIMENTARY SPONGEWORK	SPONGEWORK	RAMIFORM & SPONGEWORK CAVES

191
192 **Figure 2.** Relationship between recharge, dominant porosity, and the patterns of karst networks
193 that develop (from Palmer, 1991).

194
195

196   Rocks with high primary porosity, as found in eogenetic karst, preferentially develop
197 spongework caves (Palmer, 1991), which are often isolated voids that are not connected into an
198 integrated conduit flow system (Vacher and Mylroie, 2002). Examples of such dissolutional
199 voids include flank margin caves and "banana holes" that develop in carbonate island karst
200 (Breithaupt et al., 2021; Mylroie and Carew, 1990; Vacher and Mylroie, 2002). In such settings,
201 the locations of dissolutional voids may be controlled by zones of mixing (Mylroie and Carew,
202 1990) or by biological CO_2 production (Gulley et al., 2016, 2015). Consequently, voids
203 frequently develop near the water table, where vadose zone CO_2 can boost dissolution rates
204 (Gulley et al., 2014), or in zones of freshwater-saltwater mixing (Mylroie and Carew, 1990).
205 While evolution of such voids produced by local mixing or CO_2 production may enhance local
206 hydraulic conductivity and focus porous media flow toward enlarging voids (Mylroie and Carew,
207 1990; Vacher and Mylroie, 2002), it is less common for these processes to develop regionally
208 integrated conduit systems (Palmer, 1991). However, long-range conduit connectivity that does
209 develop in eogenetic karst is commonly associated with sinking streams (Martin and Dean, 2001;
210 Monroe, 1976), reversing springs (Gulley et al., 2011; Moore et al., 2010), or large recharge

211 areas, as found in the Yucatan Peninsula of Mexico (Back et al., 1986) and on large carbonate
212 islands (Larson and Mylroie, 2018).

213 The primary porosity of carbonate rocks also impacts the magnitude of water exchange
214 between conduits and the porous matrix. The matrix component is often considered negligible in
215 models of flow and transport in telogenetic karst aquifers (Peterson and Wicks, 2005). However,
216 in eogenetic karst, with high matrix porosity, transient head conditions within conduits,
217 combined with the relatively high permeability of the matrix, can produce substantial exchange
218 flows between the conduits and matrix, analogous to hyporheic exchange within rivers (Martin
219 and Dean, 2001). Such exchange flows may dampen the hydraulic response of karst aquifers,
220 which are typically flashy (Florea and Vacher, 2006; Spellman et al., 2019). The loss of water
221 from conduits into small intergranular matrix porosity increases surface areas available for
222 dissolution reactions. In some cases, dissolution by exchange flow may be the primary factor
223 driving evolution of connectivity within a karst aquifer (Gulley et al., 2011; Moore et al., 2010).
224 Exchange flows are also important drivers of a variety of other biogeochemical reactions, in
225 large part because of their control of redox conditions as water equilibrated with atmospheric
226 oxygen and elevated in dissolved organic carbon is injected into reducing water stored in matrix
227 porosity (Brown et al., 2014; 2019; Flint et al., 2021). Such exchange flows can occur both
228 between conduits and matrix and between rivers and the surrounding aquifer.

229 ## 2.2 Sources of undersaturation and dissolution

230 In the classic conceptual model of karst development, calcite dissolution is driven by
231 carbonic acid. Meteoric water dissolves CO_2 within the atmosphere and soil and carries this CO_2
232 downward into the rock, dissolving carbonate minerals along its way (Adams and Swinnerton,
233 1937). Karst developed by such processes is often referred to as epigene karst, indicating its
234 close relationship to surface processes, in contrast to hypogene karst, which develops at depth.
235 This classic conceptual model has been expanded in several ways, particularly as it relates to the
236 sources of CO_2. In some karst settings, CO_2 concentrations are higher at depth than within the
237 soil, suggesting CO_2 production deep within the vadose zone, perhaps as the result of the
238 remineralization of particulate organic matter that has infiltrated to depth (Atkinson, 1977b;
239 Mattey et al., 2016; Noronha et al., 2015; Wood, 1985) or the influence of deeply rooted
240 vegetation (Breecker et al., 2012).

241 In addition to carbonic acid, carbonate dissolution can be driven by a variety of other
242 acids, with sulfuric and nitric acids being the most common. Sulfuric acid is widely cited as a
243 source of dissolution in hypogenic speleogenesis (Egemeier, 1988; Engel et al., 2004), in marine
244 carbonate sediments (Beaulieu et al., 2011; Torres et al., 2014), and in landscapes affected by
245 acid rain (Shaughnessy et al., 2021). Sulfuric acid can be produced through fossil fuel
246 combustion, especially coal (Irwin and Williams, 1988). Sulfuric acid is also produced where
247 oxygen-rich air or water encounters reduced sulfur species such as pyrite in sedimentary rocks or
248 H_2S produced by coupled microbial organic carbon oxidation and sulfate reduction. Carbonate
249 dissolution can also occur by nitric acid produced during microbial nitrification or industrial
250 processes. Nitric acid production has been enhanced by anthropogenic production of reactive
251 nitrogen species (Galloway, 1998; Galloway et al., 2008), for example by chemical fertilizer use
252 in intensive agriculture and partial oxidation of atmospheric N_2 in internal combustion engines
253 (Gandois et al., 2011; Perrin et al., 2008). Organic acids may also be important drivers of
254 dissolution in some carbonate settings, although their concentrations are commonly lower than
255 concentrations of sulfuric or nitric acids (Jones et al., 2015). High concentrations of organic
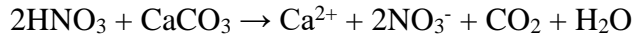
256 acids have been suggested to cause rapid carbonate dissolution in a temperate rainforest setting
257 (Allred, 2004; Groves and Hendrikson, 2011).

258   The source and type of acid causing carbonate dissolution is critical to global carbon
259 cycling (Martin, 2017). Carbonate dissolution by carbonic acid is neutral with respect to long-
260 term atmospheric CO_2 concentrations, because CO_2 consumed during weathering, $CO_2 + H_2O +$
261 $CaCO_3 \rightarrow Ca^{2+} + 2HCO_3^-$,

262   is balanced by CO_2 released during marine carbonate precipitation,

263          $Ca^{2+} + 2HCO_3^- \rightarrow CaCO_3 + CO_2 + H_2O$.

264   In contrast, dissolution of carbonates by sulfuric or nitric acids results in a net flux of
265 CO_2 to the atmosphere (Martin, 2017), with

266

267          $H_2SO_4 + 2CaCO_3 + H_2O \rightarrow CaCO_3 + CaSO_4 * 2H_2O + CO_2$.

268          $2HNO_3 + CaCO_3 \rightarrow Ca^{2+} + 2NO_3^- + CO_2 + H_2O$

269

270 Considerable work over the last two decades has focused on hypogene speleogenesis, in which
271 water undersaturated with respect to bedrock minerals forms at depth and is carried to the surface
272 with regional groundwater flow (e.g., Klimchouk, 2007; Palmer, 1991; Klimchouk et al., 2017).
273 Undersaturated water may form through many mechanisms, including cooling of rising thermal
274 waters, oxidation of reduced sulfur species, deep sources of CO_2, and mixing of waters with
275 different salinity or pCO_2. Dissolution deep within a karst aquifer may develop porosity that is
276 disconnected from points of surface recharge, forming isolated porosity rather than regionally
277 integrated flow networks. Alternatively, dissolution where deep and meteoric water mix may
278 develop integrated flow networks if the pore spaces become linked. Karst conduit networks
279 formed by hypogene processes typically develop complex mazes or ramiform passages, with less
280 tendency toward the dendritic flow patterns common in epigene karst settings (Palmer, 1991).
281 Porosity that develops in the deep subsurface may serve as a template for epigenetic karst
282 processes when exhumation due to erosion brings that porosity closer to the surface (e.g.,
283 Tennyson et al., 2017; Klimchouk et al., 2023).

284   2.3 Climate

285   Climatic factors impact the rate and forms of karst development (Lehmann, 1936). A
286 theoretical relationship for the maximum possible rate of karst denudation (D_{max}), based on
287 equilibrium carbonate chemistry (White, 1984), provides a first order estimate of the impact of
288 climate factors on rates of carbonate denudation,

289

290

291          $$D_{\text{max}} = \frac{M}{\rho}[Ca]_{eq}(P - E) = \frac{M}{\rho}\left(\frac{K_c K_1 K_{CO_2}}{4K_2 \gamma_{Ca} \gamma_{HCO_3}^2}\right)^{\frac{1}{3}} pCO_2^{\frac{1}{3}}(P - E) \qquad (1)$$

292

293 where D_{max} is in units of mm/kyr, ρ is rock density in g/cm^3, $[Ca]_{eq}$ is the equilibrium
294 concentration of calcium in mol/L, K_c, K_1, K_{CO2} and K_2 are temperature-dependent equilibrium
295 constants of the carbonate system in units of mol/L and atm, pCO_2 is the partial pressure of CO_2

296 in atm, γ_{Ca} and γ_{HCO3} are the activity coefficients of calcium and bicarbonate, respectively, which
297 are often approximated as one, M is the molar mass of $CaCO_3$ (100 g/mol), and $P - E$ is
298 precipitation minus evapotranspiration in mm/yr. Equation 1 shows the three main contributors
299 to climate-driven differences in carbonate denudation rates: 1) changes in the equilibrium
300 constants with changing temperature, 2) differences in pCO_2, which are strongly related to
301 temperature, and 3) water availability. Among these three factors, water availability plays the
302 strongest role in producing global variation in chemical denudation rates (Ryb et al., 2014; Smith
303 and Atkinson, 1976). Well-developed karst surface features are less common within hot and arid
304 settings or cold settings where water is rarely present in a liquid state (Ford and Williams, 2007).
305 When karst surface features are present in such settings, they are sometimes inherited from
306 landscapes that developed in past conditions that were wetter.

307 As temperature increases, solubility of calcite decreases, largely because of the decreased
308 solubility of CO_2. However, carbonate mineral dissolution rates increase with warmer
309 temperatures (Plummer et al., 1978). Elevated dissolution rates decrease the time required to
310 reach equilibrium within the CZ, and thus faster kinetics lead to more dissolution within the near
311 subsurface (Gabrovšek, 2009). In addition, soil pCO_2 increases with increased temperature as
312 biological activity increases (Drake, 1980). These two competing effects, of decreasing solubility
313 and increasing pCO_2 with increasing temperature, are thought to produce the observed
314 boomerang shape between $Ca^{2+} + Mg^{2+}$ concentrations and temperature within world rivers, with
315 a peak in carbonate weathering intensity around a temperature of 10° C (Gaillardet et al., 2019).
316 While a substantial body of work examines fluxes of solutes from carbonate basins and uses
317 these to estimate average denudation rates (e.g., Erlanger et al., 2021; Gunn, 1981; Lauritzen,
318 1990) the role of kinetics in partitioning dissolution within the subsurface remains an area for
319 further study.

320 While, broadly speaking, the impacts of climate on karst processes are well-understood,
321 many open questions remain. For example, polygonal or cockpit karst develops preferentially in
322 the humid tropics, whereas doline karst is more typical of humid temperate regions, and the
323 reason for this difference is unclear (Ford and Williams, 2007). Interactions between climate and
324 biological processes may be an important driver in the evolution of these landscapes.

325 2.4 Vadose zone gases and open vs. closed system weathering

326 Vadose zone gases, particularly CO_2 and O_2, play an important role in weathering
327 processes (e.g., Brantley et al., 2013; Kim et al., 2017). These gases are derived from Earth's
328 atmosphere as a primary source, although CO2 concentrations can be elevated in the vadose zone
329 due to root respiration and oxidation of organic matter (Kim et al., 2017; Wood and Petraitis,
330 1984). Gases are often assumed to be transported by diffusion in the vadose zone. However,
331 connectivity among solutionally enlarged fractures and larger conduits in karst systems enables
332 advective gas flows. Advection is forced by density contrasts between surface and subsurface air,
333 largely through temperature variations at daily and seasonal time scales (Covington, 2016;
334 Covington and Perne, 2015; Sanchez-Cañete et al., 2011), that drive seasonal and diurnal
335 changes in subsurface gas concentrations (Benavente et al., 2010; Gulley et al., 2014; Kowalczk
336 and Froelich, 2010; Lang et al., 2017; Mattey et al., 2016; Milanolo and Gabrovšek, 2009;
337 Sekhon et al., 2021; Spötl et al., 2005; Wong et al., 2011). These variations are likely to extend
338 throughout the vadose zone, even where it may be thick because of deep groundwater tables
339 (Benavente et al., 2010; Covington, 2016; Mattey et al., 2016). In some cases, soil and the
340 shallow subsurface may be aerated from below rather than directly from the atmosphere (Faimon
341 et al., 2020). The ventilation through conduit systems, and the linked changes in vadose water

342   chemical compositions and compositions at the water table, can thus provide controls on the
343   spatial and temporal patterns of dissolution and precipitation of calcite (Covington et al., 2021;
344   Covington and Vaughn, 2019; Gulley et al., 2014; Houillon et al., 2017; Spötl et al., 2005; Wong
345   et al., 2011). Similar processes can impact CO_2 gas fluxes from, and carbonate weathering
346   patterns within, the soil (Roland et al. 2013).

347   Weathering of carbonate minerals is often approximated as proceeding under open or
348   closed system conditions with respect to a CO_2 gas phase. Under open system conditions, the
349   solution is in contact with a large reservoir of CO_2 and evolves at fixed pCO_2, dissolving more
350   CO_2 from the gas phase as CO_2 is consumed by carbonate dissolution. Under closed system
351   conditions, the solution is isolated from the gas phase, and pCO_2 decreases as carbonate
352   dissolution proceeds. Open and closed conditions are partly dictated by the water saturation state
353   of the pore spaces, with complete water saturation producing closed conditions. Whether
354   carbonate dissolution proceeds under open or closed conditions impacts both the rate of
355   weathering processes (Buhmann & Dreybrodt, 1985a; Buhmann & Dreybrodt, 1985b) and trace
356   element concentrations and isotopic compositions of dissolved species (Hendy, 1971; Stoll et al.,
357   2022). A global study of spring water chemistry suggests that, on average, spring chemistry in
358   carbonate regions is well-explained by weathering under conditions that are open to soil CO_2
359   (Romero-Mujalli et al., 2019).

360   The impact of carbonate weathering processes on the isotopic composition of
361   speleothems was first investigated in the seminal work of Hendy (1971). Subsequent studies built
362   on this model to discern the effects of prior calcite precipitation, which impacts trace element
363   concentrations, and kinetic fractionation, which impacts stable isotope ratios, to confidently
364   isolate climate signals from speleothems (e.g., Fohlmeister et al. 2011; Fohlmeister et al., 2020).
365   The primary goal of these models is to illustrate the potential of speleothems to track changes in
366   the climate. However, such studies also help us to better understand local hydrological processes
367   within the epikarst that are sensitive to open and closed system conditions and pore spaces in the
368   CZ (Stoll et al., 2012). Recent work goes beyond the open/closed system framework and
369   employs a reactive transport model to simulate carbonate weathering processes and gas transport
370   in the carbonate CZ (Druhan et al. 2021; Oster et al., 2021). Such approaches provide a
371   promising new avenue for future research on carbonate CZ processes. Lastly, to investigate the
372   open versus closed system paradigm, variation in dead carbon fraction, the fraction of old,
373   radiocarbon dead C derived from bedrock, and Li isotopes of speleothems provide additional
374   constraints on the relationship between climate and weathering. Dead carbon fraction in
375   speleothems is primarily controlled by rates of limestone dissolution. High dead carbon fraction
376   is typically indicative of closed system conditions during periods of increased hydrological
377   activity (Griffiths et al., 2012; Bajo et al., 2017), though enhanced decomposition of old,
378   recalcitrant carbon is another important source of dead carbon (Rudzka et al., 2012; Noronha et
379   al., 2015). Likewise, recent studies of Li isotopes within cave drip waters and analog
380   experiments highlight the possibility of studying silicate weathering intensity using speleothem
381   records (Day et al., 2021; Wilson et al., 2021).

382   2.5 Tectonic setting and base level

383   Tectonic uplift, sea level change, and other drivers of changes in base level provide
384   important boundary conditions for the development of karst flow networks and the resulting
385   landscapes. Karst conduit development is often focused near, or driven toward, the water table

386 (Ford and Ewers, 1979). During periods of stable base level, karst conduit networks can
387 preferentially develop within specific elevation ranges (Figures 3). Such cave levels are used to
388 date phases of river incision using cosmogenic burial dating (Granger et al., 2001; Stock et al.,
389 2005). Similarly, flat corrosion plains develop when the land surface approaches base level (Ford
390 and Williams, 2007). In contrast, where rapid uplift occurs, the resulting high relief promotes the
391 development of thick vadose zones, sometimes in excess of 2 km. In these cases, conduit
392 development may be primarily vertical, along structural features such as faults, until water
393 collects within subhorizontal conduits that drain the water laterally out of massifs into springs
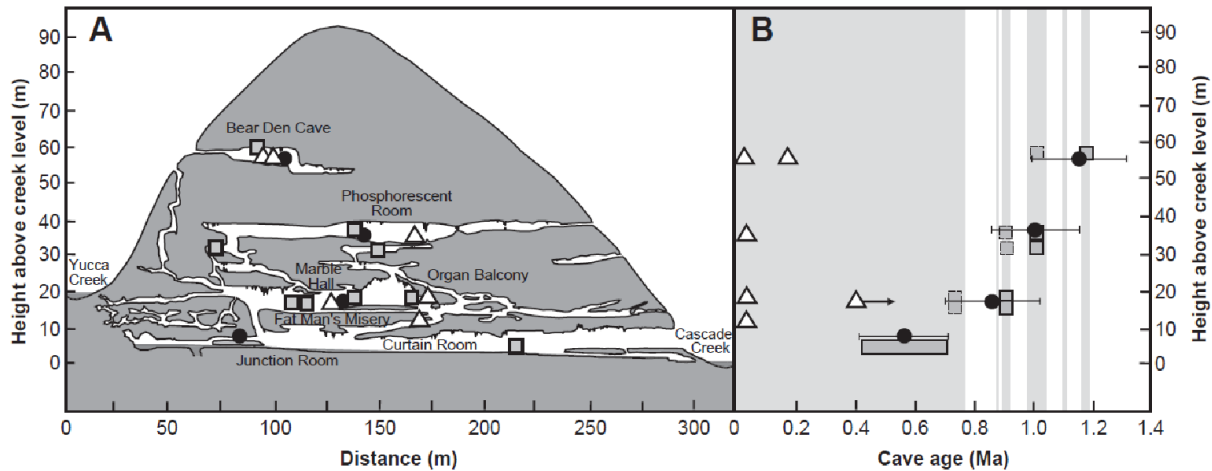394 near base level (Audra et al., 2006; Turk et al., 2014; Klimchouk, 2019).

395
396 **Figure 3.** The development of horizontal cave levels in Crystal Cave, California, in response to
397 stream incision (from Stock et al., 2005). As the surface stream incised, new levels of cave
398 passage were developed (A), rather than steepening of the existing channel, as would occur
399 during a pulse of incision in a surface stream. Locations (A) and ages (B) of cave deposits are
400 shown, including speleothem U-Th (white triangles), paleomagnetic (gray squares), and
401 cosmogenic burial (black circles) samples. The cosmogenic burial ages of coarse sand and
402 gravel are most indicative of the time when a cave passage was occupied by an active stream.

403

404 Uplift of carbonate platforms can also result from isostatic rebound caused by dissolution
405 and the resulting reduction in platform density (Adams et al., 2010; Opdyke et al.,1984). In fold
406 and thrust belts, the tendency for evaporites to act as planes of detachment frequently results in
407 the formation of anticlines with evaporite cores (Davis and Engelder, 1985), and the buoyant
408 effect of the evaporites may be an additional force contributing to uplift of the anticline (Lucha et
409 al., 2012). The juxtaposition of evaporites below uplifted, fractured carbonate-rich rocks creates
410 ideal conditions for hypogene, sulfidic karst development, as in the Central Apennines, Italy
411 (D'Angeli et al., 2019). In this setting, base level is controlled by river incision of the anticline,
412 resulting in sulfidic springs that discharge in or near river valleys. Cycles of sea level rise and
413 fall are important drivers of karst development in coastal settings, which are typical of most
414 eogenetic karst. Voids that develop at sea-level low stands are subsequently flooded during sea
415 level rise (Myroie and Carew, 1990; Smart et al., 2006; Gulley et al., 2013). Patterns of sea level
416 change can often be tracked within speleothem records (Bard et al. 2002; Roy & Mathews, 1972;
417 Surić et al., 2009).

2.6 Relative importance of chemical vs. mechanical weathering and erosion processes

Landscapes that develop on carbonate bedrock are also impacted by the types and rates of mechanical weathering and erosion. In landscapes where mechanical processes are more efficient than chemical processes, karst features will be less pronounced, even if subsurface karst flow networks are well-developed. The instantaneous rate of chemical erosion tends to be slower than the instantaneous rates of mechanical erosion processes such as fluvial incision, hillslope mass wasting, and glacial erosion. However, chemical erosion processes, both chemical denudation and dissolution-driven channel incision/conduit growth, are often relatively continuous, with chemical denudation rates depending primarily on climate (White, 1984) and dissolution rates within streams showing relatively low variability over time (Covington et al., 2015). In contrast, mechanical erosion and mass transport processes are frequently episodic. Consequently, the most extensive karst landscapes develop in humid environments where nearly continuous chemical weathering outpaces episodic mechanical processes – a tortoise and hare analogy (Simms, 2004). In environments where mechanical weathering processes are particularly effective, karst surface features may fail to develop because of the rapid breakup and accumulation of weathered rock. One such example is alpine karst settings, where frost cracking can erase surface expressions of karst (Ford, 1971).

In mixed carbonate and non-carbonate terrains, carbonates can behave either as weaker rock layers, forming topographic lows, or as strong layers that form topographic highs (Simms, 2004; Ott et al., 2019). When chemical weathering rates outpace tectonic uplift, as might be the case in either humid environments or tectonically passive settings, then carbonates tend to erode more quickly and develop lows in the topography. However, when tectonic uplift outpaces chemical weathering, as in arid or rapidly uplifting environments, then the mechanical strength of carbonates may result in the formation of topographic highs (Ott et al., 2019).

The diversion of surface water, and therefore geomorphic work, into the subsurface in sinking streams can decrease the efficiency of fluvial erosion processes. For example, karst sink points can stall the propagation of knickpoints, reducing rates at which stream profiles adjust to changes in tectonic forcing (Fabel et al., 1996). Ott et al. (2019) quantified both chemical and mechanical denudation rates in carbonates and non-carbonates in Crete, showing that mechanical processes dominate, even in the carbonates, where chemical denudation accounts for ~40% of total erosion. Their results suggest that the much greater relief that develops in the carbonates results from loss of water into the subsurface and subsequent steepening of stream channels to enable mechanical erosion rates to keep pace with uplift.

Chemical and physical processes can also interact, potentially enhancing or inhibiting each other. Experiments in subcritical cracking demonstrate unique fracture propagation behaviors in carbonates, which may relate to dissolution processes at fracture tips (Atkinson, 1984; Henry, 1978). In general, models and experiments suggest that acids can enhance fracture propagation rates in carbonate rocks (e.g., Hu & Hueckel, 2019). Roots are an important agent in mechanical breakup of rock, particularly in areas with thin regolith (Brantley et al., 2017). In carbonates, roots can take advantage of subsurface porosity generated by dissolution processes (Estrada-Medina et al., 2013), and they can also generate subsurface porosity through dissolution by root exudates or CO_2 generated by root respiration (Klappa, 1980; Rossinsky and Wanless, 1992), potentially enhancing root-driven rock fracturing. It has also been hypothesized that chemical and mechanical erosion may enhance each other within stream channels (Covington, 2014; Covington & Perne, 2015), with chemical erosion potentially loosening grains that are then removed by mechanical processes (Emmanuel & Levenson, 2014), or with mechanical

464 abrasion removing surface impurities to expose fresh weatherable carbonate minerals.
465 Mechanical weathering processes can also inhibit chemical weathering processes. For example,
466 buildup of fractured rock material on the surface, with high surface areas for reaction, may lead
467 to saturation of meteoric water before it reaches unweathered bedrock. Similarly, high sediment
468 loads within streams could armor the beds and inhibit dissolution except during periods of
469 sediment mobility.

470   2.7 Biota

471   As in the CZ more generally, the activity and spatial architecture of carbonate CZ
472 biological communities have important feedbacks to other CZ processes. Thanks to networks of
473 large voids, the carbonate CZ is distinguished by the potential for macroscopic biota including
474 fish, amphibians, and invertebrates to penetrate up to several km below the photic zone (Figure
475 4). Because both locomotion and passive transport in karst conduit networks are more
476 constrained than at the surface, carbonate CZ biological communities often show a high degree
477 of endemism. The resulting small population sizes leave carbonate CZ fauna especially
478 vulnerable to extinction (Culver & Pipan, 2013).

479   Animal communities in the subsurface can be fed either by in situ microbial primary
480 production or detrital dissolved and particulate organic carbon percolating downward from the
481 surface soil. In some cases, sedimentation of particulate organic carbon in conduits creates a
482 biological hot spot where CO_2 production from decomposition drives further carbonate
483 dissolution (Covington et al., 2013; Gulley et al.,2016). In coastal karst landscapes where
484 aquifers are density stratified and partially filled by anoxic seawater (i.e. anchialine), organic
485 matter hot spots also facilitate H_2S production from microbial sulfate reduction. As water flows
486 over the hot spot, H_2S is transported away and oxidized at redox interfaces elsewhere in the
487 network, producing sulfuric acid that drives more carbonate dissolution. A striking example of
488 this process can be observed in the Bahamian eogenetic karst. "Blue holes" (sinkholes) are
489 extremely common in the landscape and collect surface vegetation, which is deposited at the
490 bottom of the conduit in anoxic or dysoxic seawater. Tidal pumping exchanges low pH water
491 between the blue hole and matrix porosity of these eogenetic karst features, enhancing
492 dissolution reactions (Martin et al., 2012). Decomposition of the detrital plant material fuels
493 intense H_2S production and, where the H_2S diffuses into the photic zone, associated blooms of
494 sulfide-dependent photosynthetic bacteria thrive and fix additional carbon in the subsurface
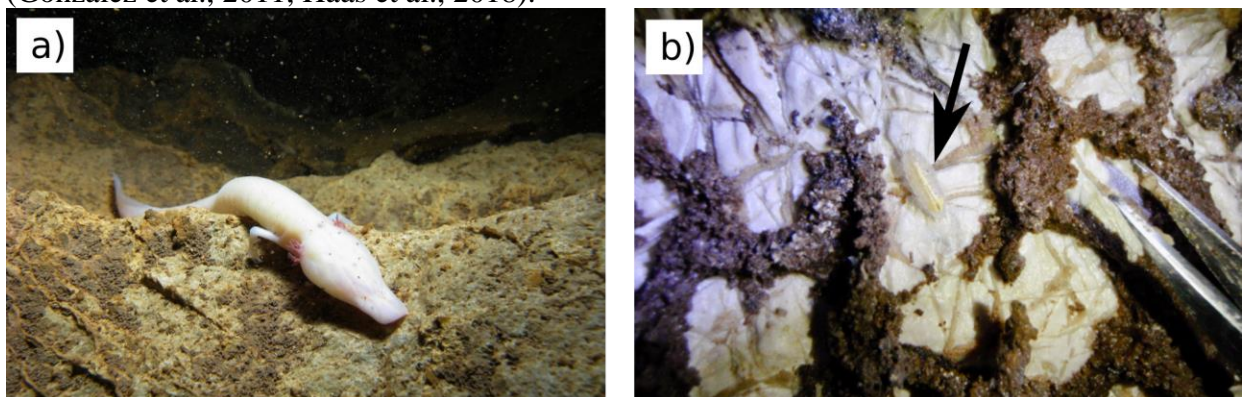495 (Gonzalez et al., 2011, Haas et al., 2018).

496

497 **Figure 4.** a) Proteus anguinus, an aquatic salamander found in the karst of the Dinaric Alps that
498 is one of the largest cave adapted animals in the world (reaching up to 40 cm in length). Photo
499 Gergő Balázs. b) A terrestrial amphipod (Androniscus sp.) scavenges among biovermiculations

500 (dark ridges) ~300 m below land surface in the Frasassi cave system, Italy. Sulfidic water
501 degassing into the cave air creates enough chemical energy to support a rich food web based
502 on microbial lithoautotrophy. Photo J. L. Macalady.

503   Vegetation on karst landscapes is affected by (1) rapid drainage and associated nutrient
504 leaching due to thin soils and large bedrock pores, (2) phosphorous scarcity due to the low P
505 content of carbonate bedrock and high phosphate complexation with abundant Ca^{2+} ions, (3)
506 strong decimeter- to meter-scale spatial heterogeneity in topography, soil and hydrologic factors,
507 and (4) limited silicate minerals, incongruent weathering, and soil formation. The plant ecology
508 of tropical and subtropical karst ecosystems has recently been reviewed in depth (Geekiyanage et
509 al., 2019). Because water in thin karst soils is in short supply, plants growing on carbonate-
510 dominated landscapes have adaptations for using alternative reservoirs of water, especially in dry
511 seasons (Figure 5). Non-tree species often have particularly dense and extensive shallow root
512 systems because they depend on soil water year-round (Ellsworth et al., 2015). Due to high
513 bedrock porosity, water stored in the vadose zone (epikarst) represents a significant alternative to
514 soil water for woody species that can penetrate into carbonate bedrock (e.g., Querejeta et al.,
515 2007). Some woody species also have specialized, long roots that reach the water table (Deng et
516 al., 2012; Swaffer et al., 2014). Adaptations for obtaining fog water (Fu et al., 2016), and a
517 drought-deciduous strategy in which leaves are shed during dry seasons (Reich and Borchert,
518 1984; Wolfe and Jursar, 2015), have also been documented in plants growing in carbonate
519 terrains.

520   Plant adaptations to obtain water resources in the carbonate CZ significantly alter the
521 hydrologic balance at depths far below the soil zone and therefore have feedbacks on weathering
522 rates and nutrient and organic carbon transport out of the system that are different than in the
523 silicate-dominated CZ (Huang et al., 2009; Dammeyer et al., 2016). Karst plant nutrient
524 acquisition strategies may also differ significantly, with potential feedback to weathering rates.
525 Plants growing on calcareous soils release organic acids from their roots in order to obtain
526 phosphate from metal complexes in the soil (Ström et al., 2005). Subsequent microbial
527 degradation of the organics further enhances CO_2 production near roots. In the presence of strong
528 topographic heterogeneity leading to soil pockets in epikarst depressions, vegetation can
529 reinforce CO_2-induced weathering hot spots in the landscape and thereby amplify dissolution
530 along certain water flow paths. A well-studied example of vegetation-mediated positive
531 weathering feedbacks can be seen in Big Cypress National Preserve, South Florida, which is
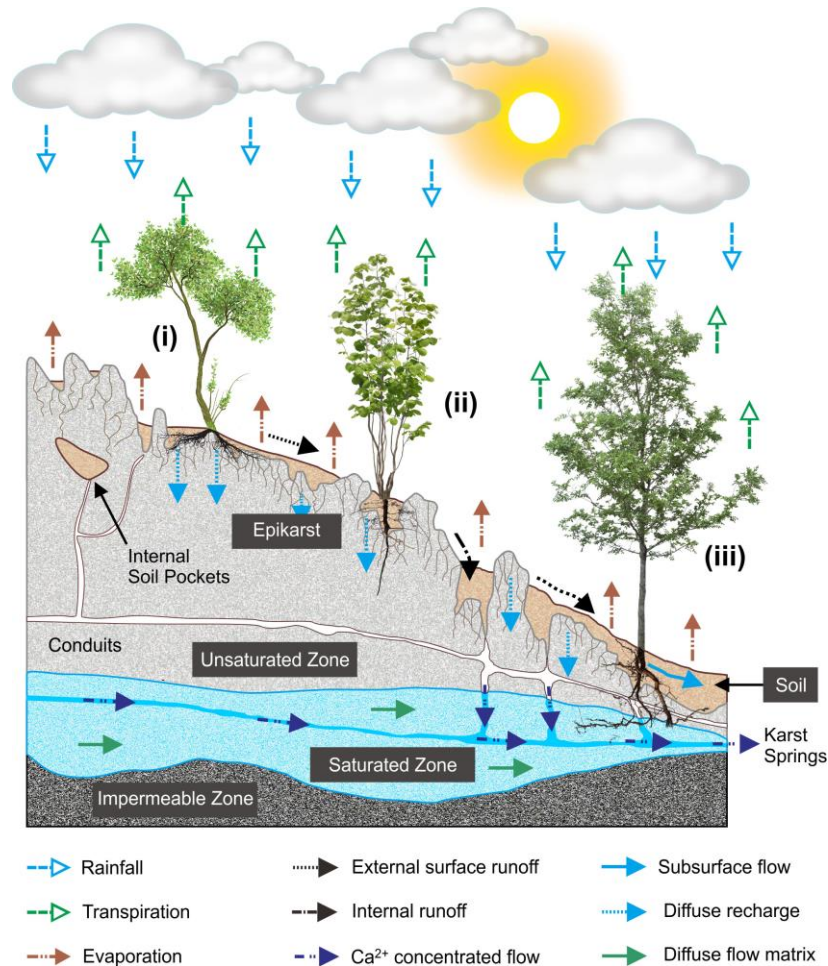532 characterized by extensive spatial patterning (Dong et al., 2019a,b).

Figure 5. Water use strategies of karst plant species in a typical karst ecosystem during the dry season; (i) soil water dependent (species that predominantly take up soil water in both the dry and wet season), (ii) epikarst water dependent (species that use both soil and water stored in epikarst in both seasons and show a major shift to epikarst water when soil water is depleted during the dry season), and (iii) groundwater dependent (species that use groundwater in addition to soil and epikarst water and show a major shift to epikarst and groundwater when soil water is depleted during the dry season). Not illustrated here are (iv) fog water dependent plants, which use fog-derived water in addition to any of the above water sources, and (v) drought-deciduous, which remain dormant by leaf shedding during the dry season. From Geekiyanage et al. (2019).

Plant roots and the microbial communities they support, including mycorrhizae, saprotrophic fungi, bacteria, and archaea have long been recognized as drivers of chemical weathering and the global carbon cycle (Beerling, 1998; Berner, 1992; Brantley et al., 2017a). Plant growth elevates soil $p\text{CO}_2$ and increases dissolved inorganic carbon (DIC) fluxes (Andrews and Schlesinger, 2001; Berner, 1997). Rooting systems (e.g., grass-, shrub- and woodlands) govern the distribution of soil carbon (both organic and inorganic), microbial biomass, and soil respiration (Billings et al., 2018; Drever, 1994; Jackson et al., 1996). For example, relatively deep root distributions in shrublands compared to grasslands lead to deeper soil carbon profiles (Jackson et al., 1996; Jobbágy and Jackson, 2000), which elevate CO_2 and therefore weathering at depth. The work described here was carried out almost exclusively at sites where the CZ is

554 dominated by silicate minerals. Only recently have similar ideas been applied to carbonate
555 terrains, particularly in connection with studies of land-use changes.

556   Changing land cover has been invoked to explain changes in carbonate weathering
557 processes. In carbonate terrains, carbon weathering fluxes have been found to be maximized in
558 grasslands as compared to shrub, managed crop, soil denuded of vegetation, or bare rock
559 dominated landscapes (Zeng et al., 2017). This optimization results from greater pCO_2 and
560 greater depths of water penetration in grasslands as compared to other land cover types. Woody
561 vegetation encroachment into grasslands underlain by carbonate systems causes shifts in flow
562 paths, groundwater solute concentration, and the timing of solute delivery to streams as inferred
563 from reactive transport models and observed changes in stream and groundwater chemical
564 compositions (Sullivan et al., 2019), with deep root systems regulating how much CO_2 is
565 transported downward to the deeper carbonate-rich zone (Wen et al., 2020). Changes in pCO_2 as
566 a response to shifts in vegetation can also be discerned through ^{13}C variability in speleothems.
567 Lechleitner et al. (2021) show that an increase in soil gas pCO_2 is recorded in speleothem carbon
568 isotope ($\delta^{13}C_{spel}$), which may retain information on soil respiration. Similarly, Stoll et al. (2022),
569 attribute trends in $\delta^{13}C_{spel}$ to soil gas and bedrock dissolution. They propose that higher
570 temperatures increase vegetation productivity, thereby increasing soil CO2 production, which
571 leads to more negative $\delta^{13}C$ in speleothems.

572   Bedrock type can control plant productivity through influencing the available nutrients
573 and physical regolith structure (Hahm et al., 2014). Data from carbonate settings suggest that
574 silicate percentage is negatively correlated with the rate of water drainage from regolith and
575 positively correlated with primary productivity (Jiang et al., 2020). It is hypothesized that
576 preferential drainage features are better developed within carbonate-rich rocks and that this leads
577 to both water and soil loss into the subsurface, reducing water availability during dry periods.
578 Similarly, a global study of relationships between rock type and biodiversity in erosional
579 landscapes demonstrates that regions rich in carbonates have less vegetation and lower animal
580 richness (Ott 2020).

581

582   2.8 Humans and the carbonate CZ

583   Human activity over millennia is intimately tied to use of karst landscapes for agricultural
584 purposes, water resources, and cultural traditions (Quine et al., 2017; Stevanović, 2018; Moyes et
585 al., 2009). The study of human evolution is rooted in investigating hominin bearing fossils
586 discovered in caves (Mijares et al., 2010; Zanoli et al., 2022; Pickering et al., 2011; Sutikna et
587 al., 2016) as well as cave art (Brumm et al., 2021; Valladas et al., 2001). Excavations of fossils
588 in cave deposits continue to be a crucial tool in piecing together the history of human evolution.
589 However, destruction of cave sites through cave infilling because of construction, and visitors
590 destroying artifacts, threaten these prehistoric records. Interdisciplinary research between social
591 scientists, geographers, archaeologists, and earth scientists is required to better constrain the
592 relationships between humans and karst landscapes. Human activity through the Anthropocene is
593 negatively impacting the karst landscape (Long et al., 2021; Beach et al., 2015). This delicate
594 environment is susceptible to soil degradation, sinkhole development, groundwater
595 contamination, and depletion in groundwater levels. Globally, many regions with carbonate
596 aquifers are predicted to experience lower precipitation and higher temperatures, reducing
597 recharge and stressing available water resources (Hartmann et al., 2014). Similar to geochemical
598 processes, environmental impacts can occur more rapidly in karst and carbonate systems. The

599 consequences of human activities in the carbonate CZ are highlighted below to draw attention to
600 the vulnerability of karst.

601   Karst uplands are vulnerable to runaway degradation if trees are removed. In the absence
602 of forest vegetation protecting thin soils, rapid erosion into exposed karst fissures culminates in
603 the creation of rocky deserts where forest vegetation can no longer gain a foothold. Rocky
604 desertification has occurred in significant areas of Mediterranean Europe (e.g., the Dinaric
605 Karst), on islands such as Haiti and Barbados in the Caribbean, and especially and most recently
606 in southwestern China (Jiang et al., 2014; Green et al., 2019). Over the past 50 years, a variety of
607 human activities have played a substantial role in the expansion of rocky deserts in China
608 including fuelwood collection, development of housing and tourism, slope cultivation, and
609 animal grazing (Zhao and Hou, 2019). Populations are impacted as farmable land can switch
610 from soil covered to denuded relatively rapidly (Zhao et al., 2020).

611   Sinkholes are one of the costliest hazards in karst regions, when collapse of underground
612 voids intersects with human land use (Gutiérrez et al., 2014). Anthropogenic activities can
613 accelerate sinkhole development, through lowering of the water table, diversion of recharge into
614 karst depressions, or creation of water table fluctuations (e.g., Newton, 1987; Parise et al., 2015;
615 Waltham, 2008; Yizhaq et al., 2017). Consequently, sinkhole hazards are closely linked to
616 human activities through both water extraction and land development. These hazards may be
617 exacerbated with future climate change as carbonate regions experience lower precipitation and
618 more extreme precipitation events, further stressing water resources and creating higher runoff
619 and larger water table variation.

620   Carbonate aquifers are particularly vulnerable to contamination (e.g., Hartmann et al.,
621 2021; White et al., 2016), and because of enlarged passages a wider range of contaminants need
622 to be considered, including pathogens, contaminants sorbed to sediment particles, and trash
623 (Ford and Williams, 2007; Vesper and White, 2003). Microplastics have recently been identified
624 in karst systems, but little is known of their sources, fate and impacts (Panno et al., 2019;
625 Balestra and Bellopede, 2022). Predicting contaminant transport pathways is complicated by
626 mixing of fast and slow flow paths, reflecting a need for an improved understanding of flow
627 components and storage (Tobin et al., 2021). Furthermore, karst systems are more vulnerable to
628 changing climate regimes, which increase or decrease precipitation inputs, and may require
629 special protection measures such as larger stormwater control structures (Veni et al., 2001). The
630 heterogeneity found in karst influences the sensitivity of recharge to climate change (Hartmann
631 et al., 2017). Therefore, water management strategies designed to cope with climate change need
632 to explicitly account for the impact of heterogeneity in karst settings.

633

634 **3 The carbonate-silicate spectrum**

635   Due to fundamental differences in the properties of silicate and carbonate mineral
636 groups, the percentage and spatial distribution of carbonate minerals within parent rocks drive
637 important differences in the processes and architectures that develop as the CZ evolves. As a
638 conceptual framework, we will consider a silicate-carbonate spectrum (Figure 6), with
639 endmember landscapes completely dominated by either carbonate or silicate minerals. This
640 framework provides a link between prior CZ studies and synthesis studies yet to be carried out in
641 both carbonate and silicate-dominated sites along the spectrum. Understanding how CZ
642 dynamics and processes change along this spectrum is a crucial next step towards integrating

643 carbonate landscapes into existing knowledge of the CZ. We argue that studying the carbonate
644 CZ will also contribute to new understanding of silicate settings by comparison.

645   3.1 Silicate-carbonate mineral mixtures and distributions in the CZ

646   Within Earth's CZ, silicate and carbonate minerals occur in mixtures across a range of
647 scales, from the grain scale to stratigraphic scales (Figure 6). At the grain scale, all carbonate
648 rocks contain some percentage of non-carbonate minerals, with common constituents including
649 clays and slowly weathering silicate minerals such as quartz and feldspars (Ford and Williams,
650 2007). Silicate mineral fractions of carbonate rocks often take the form of sand- or silt-size
651 quartz grains, or nodules or beds of authigenic chert (Figure 7a). These minerals may remain as
652 lag deposits as the carbonate minerals are dissolved (Figure 7b-c). Similarly, many siliciclastic
653 rocks contain some fraction of carbonate minerals, often in the form of a cement between grains.
654 Carbonate-cemented sandstones, or impure carbonates, can form caves and karst landforms
655 through the process of phantomization (Dubois et al., 2014; Häuselmann and Tognini, 2005;
656 Kůrková et al., 2019), whereby preferential dissolution of the cement disintegrates the rock and
657 then the remaining loose sand grains are removed physically by piping (Figure 7d).
658 Counterintuitively, the effectiveness of the phantomization process is only weakly dependent on
659 carbonate percentage, and instead disintegration is largely controlled by the grain-size and
660 texture of the silicate component (Kůrková et al., 2019). This observation suggests that the
661 change of landforms and CZ architecture along the carbonate-silicate spectrum depends on
662 variables other than just the carbonate fraction of the lithology, such as how the mineral groups
663 are distributed at the grain scale.

664   In addition to mixtures at the grain scale, silicate and carbonate rocks occur as relatively
665 pure beds in layered stratigraphy (Figure 6). Terrains composed largely of carbonates may
666 contain continuous beds of non-carbonates such as chert or shale. The layering creates
667 heterogeneities in porosity and permeability, with silicate mineral layers often less permeable
668 than carbonate layers. The contrasts in permeability can create perched water tables and zones of
669 focused conduit development in the carbonate layers (Figure 7e), while the impermeable silicate
670 mineral layers tend to impede vertical flow of water. Sometimes carbonates are thinly
671 interbedded with impure carbonates, shales, or other non-carbonate rocks, creating a landscape
672 referred to as merokarst (Cvijic, 1925). Merokarst typically displays little surface topographical

673   expression of karst but may still behave hydrologically as a karst system (Brookfield et al., 2017;
674   Macpherson and Sullivan, 2019a; Sullivan et al. 2020).
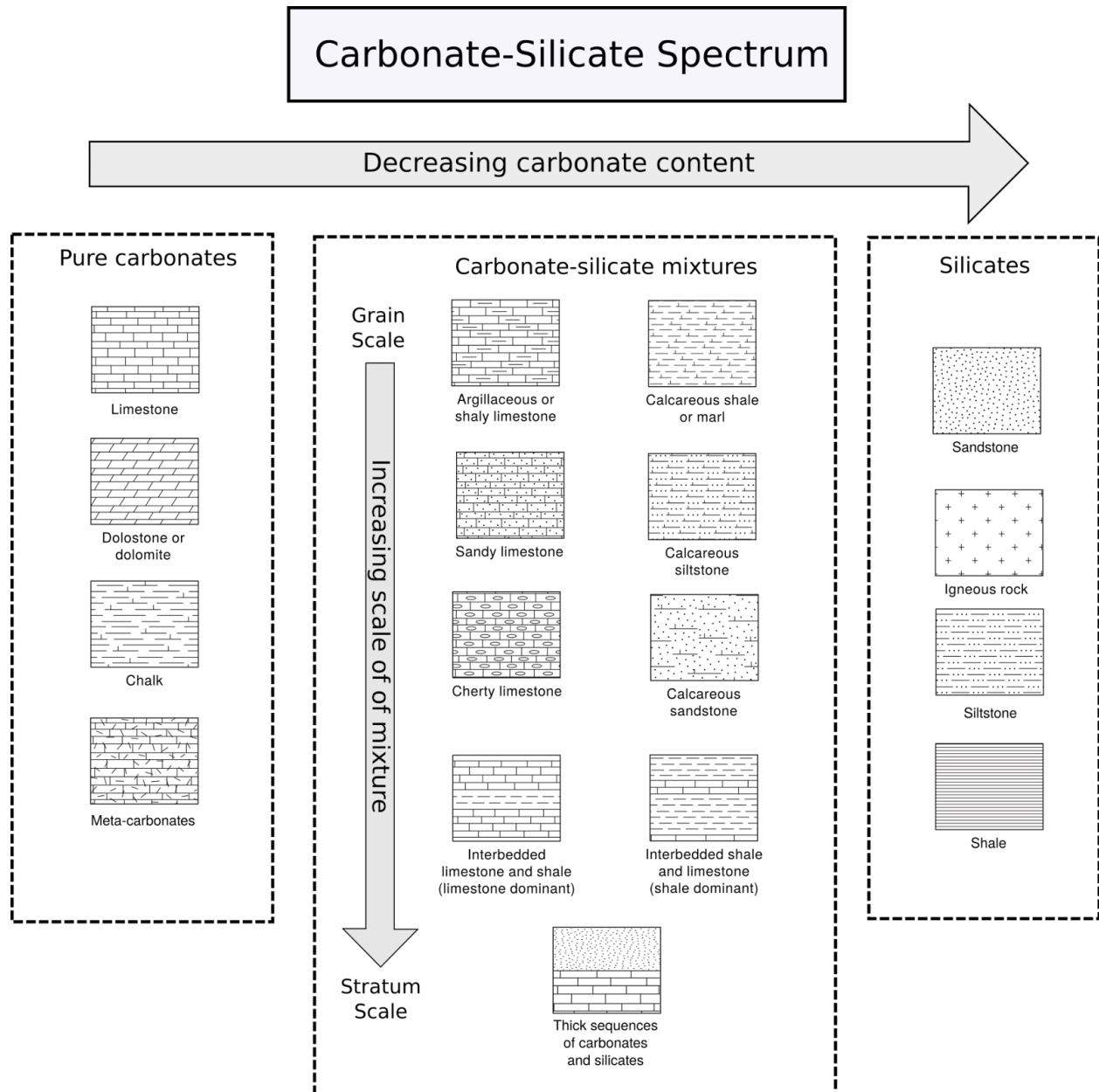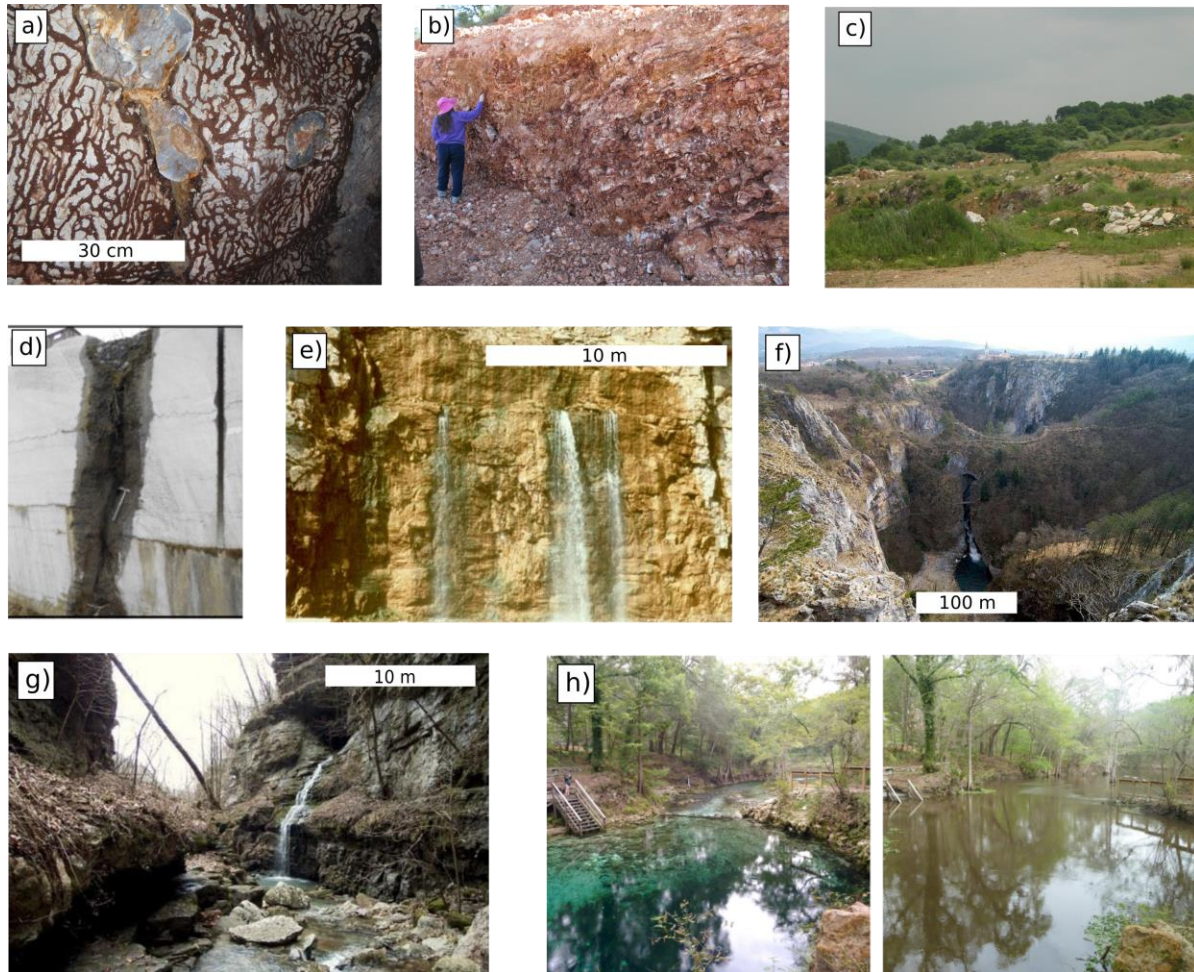
675

Figure 6. The carbonate-silicate spectrum. In addition to endmember cases of pure carbonate and silicate rocks, carbonates and silicates commonly occur as mixtures. Both the carbonate percentage and the scale over which the two mineral types mix are crucial parameters that will influence critical zone structure and evolution.

687

688
689
690 **Figure 7. Features illustrating aspects of the carbonate-silicate spectrum.** a) Differential
691 weathering of chert nodules within micritic limestone in Grotta Sulfurea, Frasassi, Italy. The
692 cave walls are colonized by microbial biofilms (biovermiculations) that prefer the carbonate to
693 the silicate surface. b) A thick regolith layer of chert and clay left behind after dissolution of the
694 Boone Limestone, Arkansas. c) Weathering residuum drapes crystalline dolomite of the
695 Cambrian Ledger Formation in Pennsylvania. d) Ghost-rock karstification (phantomization),
696 whereby weathering residuum is left behind within solutionally altered preferential flow paths,
697 near Soignies, Belgium (from Dubois et al., 2014). e) Water emerges from a bedding plane on
698 top of a chert layer within a carbonate rock, Arkansas. f) The Reka River in the classical karst
699 region of Slovenia sinks after flowing from flysch onto limestone, creating two large 160-m deep
700 collapse dolines and the upper entrance to Škocjan Caves. g) A perched spring creates a
701 waterfall at the contact where a limestone unit overlies a sandstone, Indian Creek, Arkansas. h)
702 Madison Blue Spring, Florida, an estavelle, which functions as a spring in baseflow conditions
703 (left) and reverses flow direction to receive organic-rich water from the Withlacoochee River
704 during flood events (right).

705   Thick carbonate layers may be juxtaposed laterally with non-carbonate rocks. Contacts
706 between carbonates and non-carbonates that are exposed at the surface typically form regions of
707 focused interaction between surface and subsurface hydrological, geomorphological, and
708 biological processes (Atkinson, 1977a; Brucker et al., 1972; Gulley et al., 2013; Khadka et al.,

709 2014; Martin and Dean, 1999; Palmer, 2001). When surface water flows from non-carbonate
710 onto carbonate rocks, sinking streams, blind valleys, sinkholes, and open cave shafts often
711 develop (Figure 7f). These vertical conduits capture surface runoff and route it into the
712 subsurface. Likewise, springs are common features at contacts where confining non-carbonate
713 rocks underlie carbonate rocks (Figure 7g). Such underlying confining units may produce a
714 stratigraphically determined base level for the development of karst flow systems. Springs are
715 also common where the water table intersects the land surface because erosion has removed non-
716 carbonate rocks and exposed high permeability zones in the underlying carbonates. Contact
717 zones can also host estavelles (Figure 7h), features that alternate between acting as springs and
718 sinks depending on the relative elevations of the water table and the surface water that receives
719 spring discharge. When the surface water level at the spring rises above the hydraulic head at an
720 estavelle, surface water may intrude into the spring, which can aid dissolution (Gulley et al.,
721 2011) and alter concentrations of redox sensitive solutes (Brown et al., 2019).

722 3.2 Differences between carbonate and silicate settings

723 CZ architecture and dynamics differ substantially between settings that are dominated by
724 either carbonates or silicates. Here we examine these differences, contrasting the endmember
725 cases. Less is known about how these differences emerge along the carbonate-silicate spectrum,
726 the parameters that control these changes, and whether changes occur smoothly with these
727 parameters or exhibit non-linear, threshold responses. Understanding how the CZ varies along
728 the entire carbonate-silicate spectrum is an important area for future research.

729 3.2.1 How deep is the carbonate CZ?

730 The dissolutional enhancement of permeability, and the resulting high flow velocities
731 (Worthington et al., 2016), produce rapid advection of solutes into the subsurface. After
732 development of preferential flow paths, substantial changes in flow and chemistry can be
733 expected deep within and throughout the carbonate CZ over short time periods, such as
734 individual storm events. Such variability is expected both within larger dissolutional conduits
735 (e.g., Ashton, 1966; Birk et al., 2006; Brown et al., 2014; Covington et al., 2012; Groves and
736 Meiman, 2005; Gulley et al., 2011; Liu et al., 2004; Vesper and White, 2004) and within smaller
737 dissolutionally enlarged fractures and the epikarst (Kogovšek and Petrič, 2012; Liu et al., 2007;
738 Miorandi et al., 2010; Musgrove and Banner, 2004; Tooth and Fairchild, 2003). Consequently,
739 within the carbonate CZ, surface-like geochemical conditions can occur at substantial depth and
740 at long distances from locations of point recharge. These changes deep within the carbonate CZ
741 differ from the commonly assumed base of the silicate CZ as the depth where regolith formation
742 begins (Figure 8). Thus, an important consideration in contrasting Earth's CZ in endmember
743 carbonate and silicate settings lies in the definition of the CZ itself, specifically, its lower
744 boundary, and the lower boundary's relationship with the mineralogical makeup of the CZ and
745 active circulation of water (Condon et al., 2020).

746 Riebe et al. (2017) review possible criteria for defining the base of the CZ. Ultimately,
747 they settle on an equilibrium-based definition; that is, the base of the CZ is the depth in the
748 subsurface at which meteoric water and Earth materials are at chemical equilibrium. Although
749 they do not explain why, they also note that a different definition may be needed for carbonate
750 settings. We see two ways in which the equilibrium definition might be problematic in
751 carbonates. First, given that active dissolution of calcite by meteoric water can occur at great
752 depths, up to thousands of meters (Klimchouk, 2019), the lower boundary using this definition
753 can be quite deep, leading to a picture of the CZ that differs substantially from the typical

754   hillslope catena (Figure 8). However, given that deep karst conduits can provide important
755   controls on the fluxes of water, gas, and sediment through the CZ, it seems that a holistic
756   understanding of the carbonate CZ requires an incorporation of coupling between the near and
757   deep subsurface. Therefore, the extreme depth of carbonate dissolution illustrates a meaningful
758   difference in the dynamics and processes that occur in carbonate and silicate settings.

759   Perhaps ironically, the second potential problem that we can see with the equilibrium
760   definition of the base of the carbonate CZ is that, due to rapid kinetics, meteoric water
761   equilibrates quickly with carbonates. Consequently, water may be effectively saturated with
762   calcite in the near subsurface, ending further chemical weathering. That is, the equilibrium
763   definition may specify too shallow a depth of the CZ, with a bottom boundary that is above
764   depths in which additional CZ processes occur. In fact, these two problems can be seen as
765   opposite sides of the same coin. They both result from the non-planar nature of the weathering
766   front within carbonates (Phillips et al., 2019). Although meteoric water often comes close to
767   equilibrium with calcite in the near subsurface, non-linear kinetics reduce dissolution rates as
768   water nears equilibrium with carbonate minerals, enabling undersaturated water to penetrate deep
769   into the subsurface (Dreybrodt, 1990; Palmer, 1991). Even in the absence of such non-linear
770   kinetics, flow fingering or "wormhole" development can drive undersaturated water deep into
771   dissolving fractures (Szymczak and Ladd, 2011, 2012).

772   An additional complexity is that many processes add dissolutional capacity by altering
773   equilibrium conditions in the deep subsurface. These processes include CO_2 production
774   (Atkinson, 1977b; Benavente et al., 2010; Gulley et al., 2015; Mattey et al., 2016), rising thermal
775   water that is often charged with CO_2 or other volcanically derived acids (Dublyanski, 1995;
776   Andre and Rajaram, 2005; Gary and Sharp, 2006; Klimchouk et al., 2023), mixing of surface-
777   derived meteoric water with water containing H_2S (Davis, 1980; Egemeier, 1987; Hill, 1990;
778   Jagnow et al., 2000; Palmer, 1991; Martin, 2017), mixing of water with different partial
779   pressures of CO_2 (Bögli, 1964; Wigley and Plummer, 1976), or mixing with salt water (Back et
780   al., 1986; Mylroie and Carew, 1990; Plummer, 1975). Each of these processes may alter
781   equilibrium to produce undersaturated conditions deep within the CZ. Therefore, if using an
782   equilibrium definition of the CZ, we must determine which of these equilibrium-altering
783   processes are meaningfully classified as CZ processes.

784   Despite potential difficulties outlined above, we think that an equilibrium-based
785   definition of the lower boundary of the CZ in carbonates is a reasonable starting point. A
786   working definition of the base of the CZ in carbonate settings would then be, "The depth below
787   which there is no measurable dissolution of carbonate minerals by meteoric water." This
788   definition comes with the understanding that: 1) much of the water between the surface and the
789   base of the CZ will be at or near equilibrium with respect to carbonate minerals, even though it is
790   within the CZ, and 2) some of the dissolution will be driven by subsurface acid production
791   and/or mixing of meteoric water with deeper water. When separating CZ and non-CZ processes,
792   perhaps the most difficult delineation to make is between dissolution processes that are driven by
793   proximity to Earth's surface and those which can occur at great depth from rising thermal waters,
794   H_2S-rich fluids, or volcanic production of CO_2. While many of these deeper processes may
795   create a template for further permeability development by near-surface processes as rocks are
796   exhumed, they can be considered as initial conditions for CZ development, much like the initial
797   mineralogy, fabric, and structures of the exhumed rock layers, rather than as an integral
798   component of CZ dynamics. Here, we propose that the bottom boundary of the carbonate CZ is
799   defined by feedback between dissolution and the near-surface hydrological, geomorphological
800   and biogeochemical processes. Specifically, CZ dissolution processes are those that are both

801 influenced by meteoric water and produce changes in porosity that influence the flow of meteoric
802 water.

3.2.2 The Conveyor model and CZ architecture

804   We use a conceptual model central to understanding CZ evolution within silicate terrains
805 – the CZ conveyor (see e.g., Riebe et al., 2017) – to explore differences between the CZ in
806 carbonate and silicate endmembers. Within the CZ conveyor model (Figure 8a), minerals are
807 brought upward toward Earth's surface via erosion, exposing them to physical, chemical, and
808 biological gradients. These gradients drive incongruent weathering that transforms bedrock into
809 regolith that is transported down hillslopes toward stream channels. Through the migration of
810 knickpoints, the stream channel network communicates erosion rate changes driven by tectonics
811 or isostasy upward to the hillslopes. As channels at the base of hillslopes experience a change in
812 erosion rate, hillslope topography and downslope transport of regolith adjust to accommodate the
813 change. This system reaches topographic equilibrium when fluxes of fresh rock into the CZ are
814 balanced by fluxes of solutes and sediments out of the channel network, resulting in a steady soil
815 and regolith thickness. This conceptual model, in various forms, is ubiquitous throughout CZ
816 studies (Amundson et al., 2007; Anderson et al., 2013, 2002; Brantley et al., 2017a; Heimsath et
817 al., 2020; Hilley et al., 2010; Lebedeva et al., 2010; Patton et al., 2018; Rempe and Dietrich,
818 2014; Riebe et al., 2017).

819   Arguably the most fundamental difference between the weathering of silicates and
820 carbonates is that carbonate minerals weather congruently, while silicate minerals weather
821 incongruently. Incongruent weathering produces a key aspect of the conveyor model, whereby
822 only a portion of the rock is removed in solution and the remaining sediment is transported to
823 channels via hillslopes (Figure 8a). This model thus predicts dynamic adjustment of soil and
824 regolith thickness, producing negative feedback that drives soil production and rock lowering
825 toward the average landscape erosion rate. When erosion rates increase, the down cutting of
826 channels steepens the hillslopes and thins the soils, accelerating soil production. When erosion
827 rates decrease, reduction in the rate of stream incision leads to reduction in hillslope relief,
828 accumulation of soil, and reduction of weathering rates as soil thickens (Heimsath et al., 1997).
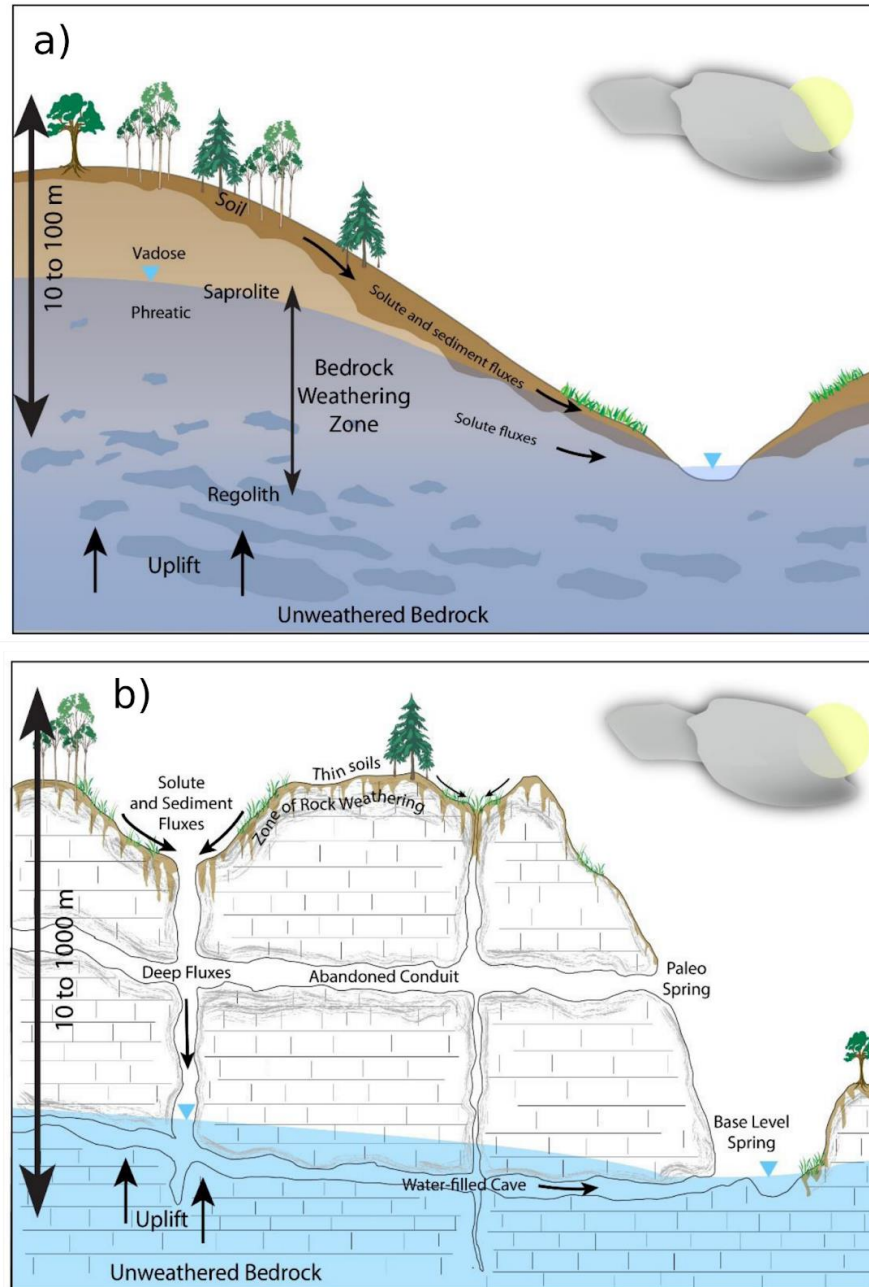
Figure 8. Carbonates and the conveyor model of the CZ. a) The conveyor model of the CZ, whereby uplift brings unweathered bedrock toward the surface. Weathering processes convert the bedrock into regolith and soil. Gravity transports sediment down the hillslopes, and stream channels carry away the solutes and sediments that are the byproducts of weathering. Communication between the hillslopes and channel network enables equilibration of the landscape to a rate of steady base level fall. b) Conceptual model of a well-developed karst in a carbonate setting. Surface drainage is limited. Congruent weathering of the carbonate rock leaves behind a thin soil. Much of the residuum from carbonate weathering may be routed through internally drained basins into the karst conduit network, potentially disconnecting hillslope response from changes in the rate of base level fall. Karst systems often respond to base level fall through the development of additional levels of conduits. Rapid carbonate weathering can occur deep within the subsurface in the vicinity of conduits and fractures.

842

843   Unlike silicate minerals, however, congruent weathering of carbonate minerals leaves
844 only minor amounts of insoluble residue and therefore little soil or regolith (Figure 8b). Soils in
845 carbonate terrains may develop largely from aeolian dust deposition (Macpherson and Sullivan,
846 2019b), and soil thickness may depend on the carbonate purity or dust delivery rate rather than
847 erosion rates such as in silicate terrains (Green et al., 2019; Moore et al., 2017). Additional
848 differences result from the greater solubility and faster reaction kinetics of carbonate than silicate
849 minerals (Plummer et al., 1979; Svensson and Dreybrodt, 1992). In actively eroding landscapes
850 that are dominated by silicates, chemical weathering fluxes are typically an order of magnitude
851 less than physical erosion fluxes (Riebe et al., 2001; West et al., 2005). At low erosion rates ($\lesssim$
852 40 mm/ka), silicate weathering is supply limited, and therefore linearly proportional to physical
853 erosion rates, whereas at high erosion rates ($\gtrsim$ 400 mm/ka), silicate weathering is kinetically
854 limited and non-linearly related to erosion rate (West et al., 2005; Gabet and Mudd, 2009). Due
855 to the rapid kinetics of carbonate dissolution, carbonate weathering is unlikely to be kinetically
856 limited. Instead, in rapidly eroding landscapes carbonate weathering is expected to be limited by
857 acid availability (Bufe et al., 2021; Gaillardet et al. 2018), also called the equilibrium limit.
858 Silicate weathering fluxes are only occasionally comparable to or larger than physical erosion
859 fluxes, primarily in low relief settings (Bouchez et al., 2014; Dellinger et al., 2017). In contrast,
860 the congruent weathering and rapid dissolution kinetics of carbonates should produce higher
861 fractions of total denudation fluxes that are in dissolved form. While few studies have attempted
862 to quantify physical erosion fluxes in carbonate landscapes (Erlanger et al., 2021; Newson, 1971;
863 Ott et al., 2019), available data suggest that chemical weathering fluxes can be comparable to
864 physical erosion fluxes, even in high relief terrain (Ott et al., 2019).

865   Feedback mechanisms between soil development and denudation may be weakened, or
866 even decoupled, within pure carbonate settings, particularly if the rate of soil development is
867 controlled by allochthonous dust input. Carbonate denudation also may be controlled more by
868 water availability and pH, rather than by topography or soil thickness as in silicate terrains
869 (Gabrovšek, 2009; Gombert, 2002; Ryb et al., 2014; White, 1984). The weakening of feedback
870 between soil formation rates and denudation rates may inhibit the approach to topographic
871 equilibrium or increase the equilibration timescale. However, equilibrium landscape
872 configurations that are entirely internal (autogenic) are also possible. For example,
873 biogeomorphic feedbacks between soil thickness, CO_2 production, and weathering rates can
874 produce equilibrium landscapes within low relief carbonate settings where the water table is near
875 the surface, such as Big Cypress Swamp in southern Florida (Cohen et al., 2011; Dong et al.,
876 2019a, 2019b). Here, modeling and field data suggest that initial development of a karst
877 depression leads to the accumulation of soil and colonization by rooting plants. As soil thickens,
878 water becomes more available, and root respiration increases, increasing the pCO$_2$ at the rock
879 surface and accelerating rates of rock weathering and depression growth. However, once
880 sufficiently thick, soil cover inhibits the delivery of CO_2 to the rock surface. Ultimately, these
881 feedbacks can produce a patterned equilibrium landscape that depends on internal controls rather
882 than external erosional or tectonic forcing.

883   Within the conveyor belt conceptual model for the silicate CZ, weathering occurs along
884 planar fronts that are subparallel to the land surface (Figure 8a). In karstic carbonate terrains,
885 weathering is focused along high permeability zones that create heterogeneous and irregular
886 weathering patterns (Figure 8b) that are rarely subparallel to the surface (Phillips et al., 2019;
887 Williams, 1985). Active weathering thus spans a range of depths, from exposed rock at the
888 surface to rock that is hundreds, or even thousands, of meters below the surface (Audra et al.,

2007; Klimchouk, 2019). The upper zone of weathering, often called the epikarst, typically has a higher degree of irregularity than the surface topography (Figure 9). This irregularity can grow over time through positive feedback resulting from flow-focusing (Klimchouk, 2004; Williams, 2008a, 1985) and generation of soil CO_2 that enhances shallow dissolution (Dong et al., 2019a; Gulley et al., 2015). The control of spatial weathering patterns in the subsurface of karst by geological structures and hydrological boundary conditions (Palmer, 1991), rather than soil properties or topography, indicates that models of carbonate CZ evolution will need to incorporate heterogeneity explicitly, as has been done in models of cave development (Dreybrodt, 1990; Gabrovšek and Dreybrodt, 2001; Groves and Howard, 1994; Hanna and Rajaram, 1998). These heterogeneities are missing from the lateral homogeneity of the conveyor belt model of the silicate CZ (Figure 8a).
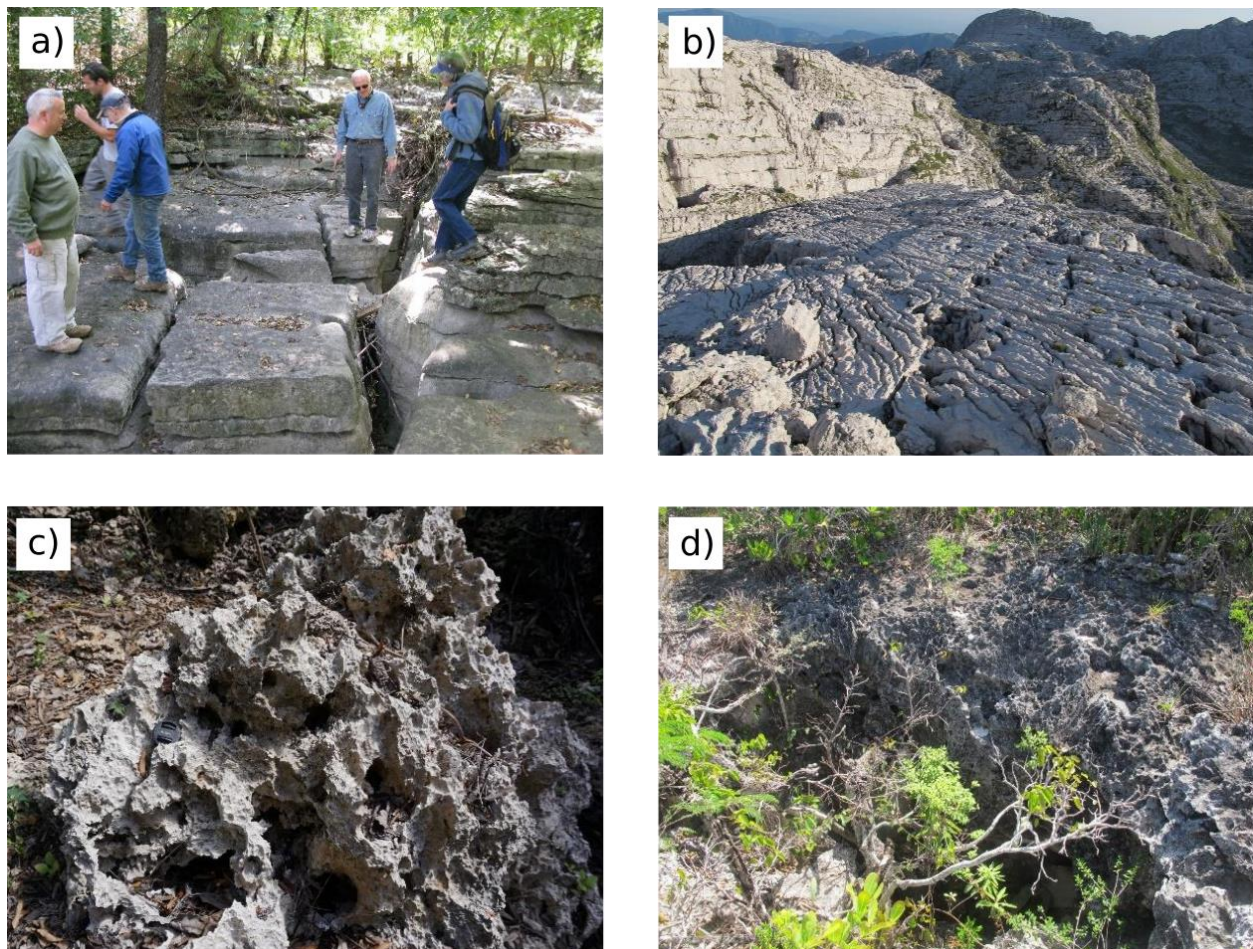
Figure 9. Weathering surfaces in carbonate terrains. a) Weathering along orthogonal joints in the St Joe Limestone in northern Arkansas. Floodwaters from a dam spillway have eroded the soil and exposed the weathering epikarst. b) Karren and epikarst surface on Dachstein Limestone on Mt. Kanin, Slovenia. c) Intense solutional weathering on an exposed piece of young, porous carbonate in Zanzibar. d) Thin soil and vegetation drape the weathering surface of young carbonates on San Salvador Island, Bahamas. In the center of the photo is the entrance of a 7-meter-deep solution shaft.

911   The focus of dissolution along high permeability zones in carbonate terrains causes an
912 additional breakdown of the coupling between tectonic uplift and erosion rates found in the
913 conveyor model. In the conveyor model, surface streams transport the sediment and solutes
914 delivered to them by hillslopes (Figure 8a), enabling landscape-wide equilibration of erosion to
915 uplift. However, surface streams are largely absent within a mature karst terrain, as all runoff and
916 sediment generated near the land surface is diverted into the karst conduit system through closed
917 basins (dolines or sinkholes) (Figures 8b, 10) (Ford and Williams, 2007). Thus, if the conveyor
918 model of the CZ is transposed from silicate to carbonate terrains, dolines would represent
919 hillslopes, and conduits would represent stream channels (Figure 8b). Even with relatively little
920 relief (tens of meters), the hillslopes of dolines may be decoupled from base level, as dolines
921 typically feed water and sediment vertically into the subsurface along solutionally enlarged
922 fractures and conduits (Brucker et al., 1972; Klimchouk, 2004; Palmer, 1991; Williams, 1985).
923 Therefore, many of the "hillslopes" of karst terrains terminate at the tops of vertical subsurface
924 channels.

925   Even in the case of dolines feeding into subhorizontal conduits, changes at base level
926 may not propagate through karst conduit networks as they do through surface channel networks.
927 First, the geometry of karst conduits, including the profiles of the streams within them, are often
928 controlled by structural heterogeneities in the rock, such as bedding partings and fractures
929 (Filipponi et al., 2009; Lowe and Gunn, 1997; Palmer, 1991). Therefore, the initial profiles of
930 streams within karst conduits may be far from the equivalent equilibrium channel morphologies
931 (e.g., slope-discharge relationships) that would be expected within surface stream channels.
932 Second, under conditions of rapid base level change, karst systems often respond by the
933 development of new levels and abandonment of old cave channels (Figures 3 and 8b) (Audra et
934 al., 2007; Gabrovšek et al., 2014; Granger et al., 2001; Stock et al., 2005; Wagner et al., 2011),
935 rather than through the propagation of knickpoints. Similar shifts in cave development in coastal
936 carbonate settings result from variations in sea level (Florea et al., 2007; Gulley et al., 2013). The
937 development of new levels within karst systems may often be sufficiently fast that stream
938 profiles within karst conduits do not have time to adjust their long profiles and erosion rates to
939 accommodate changes in the rate of base level rise and fall.

4 A dissolving and leaky conveyor

941   The most basic concepts within the conveyor model remain intact within carbonate
942 settings – rock is uplifted toward Earth's surface, it undergoes weathering, and the products of
943 weathering are transported seaward. However, the details of the conceptual model need revision
944 because of two fundamental ways in which carbonate settings diverge from the standard
945 conveyor model. First, congruent weathering causes a large fraction of the total weathering flux
946 to be exported from the system in a dissolved form. Second, the development of integrated
947 subsurface drainage networks with high permeability and rapid, often turbulent, flow, allow solid
948 weathering products to be transmitted to base level via subsurface conduits rather than along
949 hillslopes and surface streams. Each of these two factors can be quantified using a dimensionless
950 weathering flux fraction that varies between zero and one. The first factor, the importance of
951 dissolved flux is quantified by the W/D ratio, which has been studied in many silicate terrains
952 (e.g., Bouchez et al., 2014; Dellinger et al., 2017; Riebe et al., 2001; West et al., 2005), with

953
$$F_{dissolved} = \frac{W}{D} = \frac{W}{W+E},\qquad\qquad(2)$$

954   where W is the dissolved weathering flux, E is the physical erosion flux, D is the total denudation
955   flux (dissolved and solid), and $F_{\text{dissolved}}$ is the fraction of dissolved flux, and where all fluxes have
956   dimensions of M L^{-2} T^{-1}. The second factor, related to subsurface transfer of the solid erosion
957   flux, is quantified by

958
$$F_{solid,sub} = \frac{E_{sub}}{E_{sub} + E_{surf}}, \qquad\qquad (3)$$

959   where E_{sub} is the physical erosion (solid) flux that transits through subsurface conduits, E_{surf} is
960   the physical erosion flux that remains near the surface and is transmitted to base level via
961   hillslopes and surface channels, and $F_{\text{solid,sub}}$ is the fraction of the solid erosion flux that transits
962   through subsurface conduits.

963   We consider two modified versions of the conveyor model, which we call the "dissolving
964   conveyor" (where $F_{\text{dissolved}}$ is large) and the "leaky conveyor" (where $F_{\text{solid,sub}}$ is large). Both
965   modifications of the original conveyor model result in a weakening of the negative feedback
966   mechanisms that drive weathering rates toward uplift rates and produce equilibrium landscapes.
967   The dissolving conveyor describes settings where the dissolved fraction of the total seaward flux
968   of weathering products is close to one, meaning that most weathered materials exit the system as
969   solutes. While in silicate terrains $F_{\text{dissolved}} \sim 1$ can result from low relief and very low rates of
970   physical evacuation of weathering byproducts, in pure carbonates this can result from congruent
971   weathering and consequent lack of solid weathering byproducts. In this case, the buildup of soil
972   and regolith is insufficient to retard denudation. If tectonic uplift is rapid, topography may
973   become extremely steep, until mechanical weathering and erosion processes match uplift (Ott et
974   al., 2019). In this case, the system would be driven away from the dissolving conveyor state as
975   solid material export increases due to steepened terrain. In contrast, where uplift rate is low, the
976   lack of negative feedback enables the development of karst planation surfaces (e.g., Krklec et al.
977   2022; Simms, 2004; Smart et al. 1986). Here, surface denudation is not arrested until the land
978   surface approaches base level and the water table.

979   The leaky conveyor describes settings where the fraction of solid weathering products
980   transported through the karst conduit network is high ($F_{\text{solid,sub}} \sim 1$), meaning that both solid and
981   dissolved weathering materials transit through the subsurface to base level rather than down
982   hillslopes and stream channels. This fraction should govern the ability of karst landscapes to
983   develop, with high subsurface flux fractions producing landscapes dominated by dolines (Figure
984   10) and lacking integrated surface drainage networks. Again, this subsurface transport weakens
985   feedback between uplift, weathering, and erosion, as base level changes may not communicate
986   through the subsurface as they would in a surface stream network. In such cases, autogenic
987   processes may drive patterns in topography and regolith thickness (e.g., Dong et al., 2018) rather
988   than external forcing by tectonics.

989   While each of these modified models can be considered separately, there is likely a
990   strong correlation between the two governing dimensionless fractions in real landscapes. Settings
991   with a higher fraction of dissolved weathering fluxes will tend to have a higher percentage of
992   weathering fluxes transiting through the conduit network. In these settings, karst conduit
993   networks will be better developed than in settings where solid weathering products dominate,
994   because the buildup of solid weathering products can plug conduits and impede conduit growth.
995   Importantly, both weathering flux fractions could be quantified via field studies. While there are
996   some studies that quantify the relative importance of chemical and physical denudation fluxes

997 from carbonate landscapes (e.g. Erlander et al., 2021; Ott et al., 2019), we are not aware of any
998 studies that have quantified surface vs. subsurface fluxes. The controls on both flux fractions are
999 currently poorly constrained in carbonate settings. While position on the carbonate-silicate
1000 spectrum is undoubtedly important, other factors, such as climate and tectonics, should also
1001 impact these flux fractions. Further work is also needed to elucidate the impacts that these
1002 weathering flux fractions, and their external controls, have on CZ architecture, dynamics, and
1003 resilience.

1004
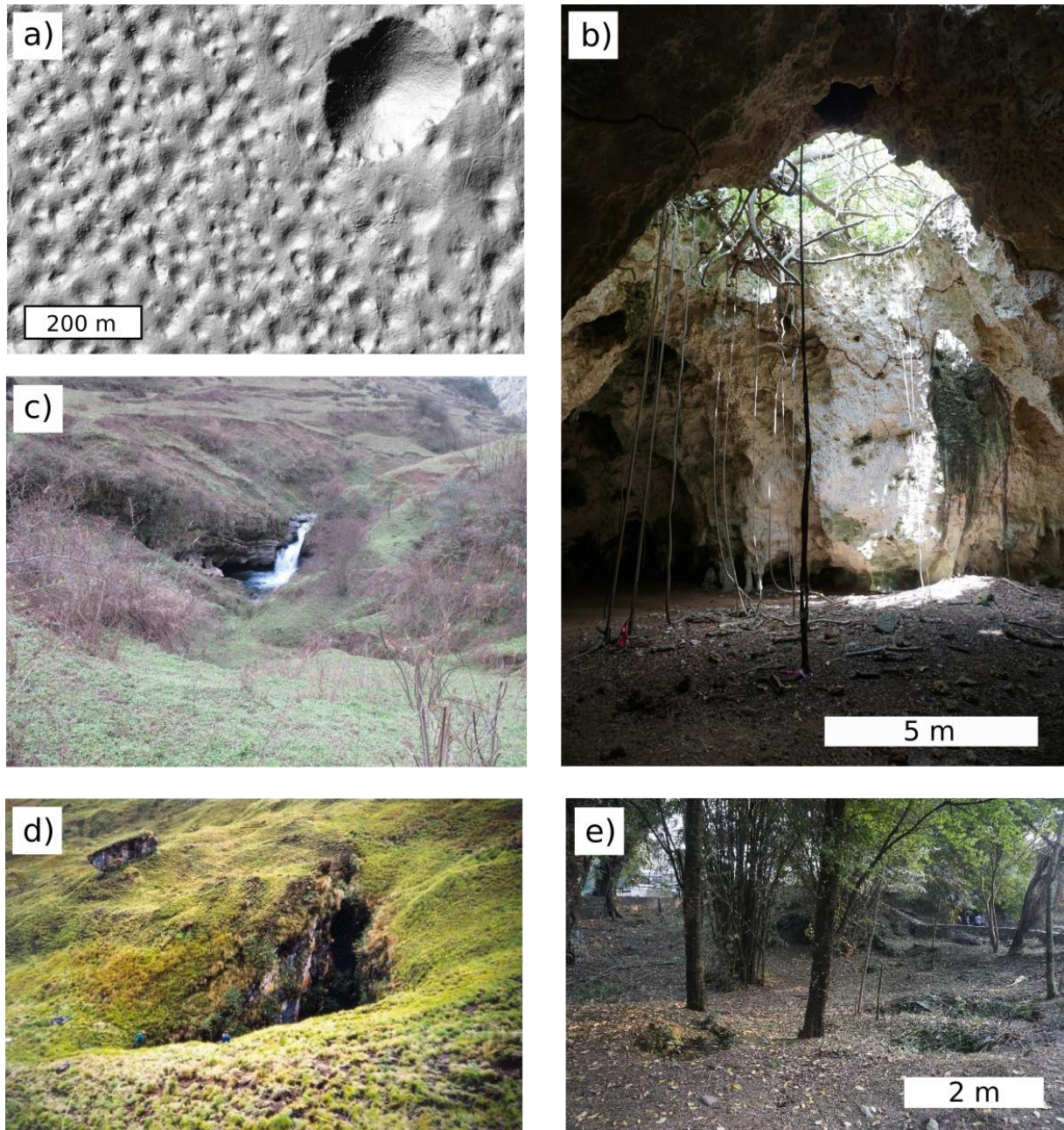1005 **Figure 10.** Dolines/sinkholes and shafts in karst terrains. a) A lidar hillshade of solution dolines,
1006 and a collapse doline, on Logaška Planota, Slovenia. b) Vegetation hangs into a collapse doline
1007 in a cave system on the island of Zanzibar. c) A stream channel within a blind valley sinks into a
1008 doline near the contact with carbonate rocks in Wulong County, China. d) A 60-meter-deep

1009   vertical shaft breaches a hillslope in the Andes of northern Peru (note cavers for scale). e) Small
1010   solutional dolines developed in a calcite-cemented conglomerate near Pokhara, Nepal.

5 Conclusions

1012   Carbonates underlie a substantial portion of Earth's surface and represent an important
1013   fraction of Earth's CZ, providing crucial water resources and ecosystem services to more than a
1014   billion people. Our current state of knowledge suggests that the congruent weathering, high
1015   solubility, and fast kinetics of carbonate dissolution lead to altered rates and patterns of CZ
1016   evolution in carbonates compared to silicate settings. When landscapes develop in relatively pure
1017   carbonate rocks, karst systems typically form, producing large contrasts in subsurface
1018   permeability and long-range subsurface connectivity that enable rapid fluxes of water, solutes,
1019   sediment, and gases through the CZ along routes of preferential flow. Direct relationships
1020   between biological CO_2 production and carbonate weathering by carbonic acid mean that
1021   production of porosity in the subsurface may be tied to biological processes in carbonates,
1022   potentially enabling carbonate-specific feedback loops between CZ development and ecosystem
1023   form and function. Because of the rapid kinetics of calcite dissolution, shifts in system dynamics
1024   and structure due to changes in ecology, land use, or climate may also be rapid.

1025   These differences show that conceptual models developed to understand CZ architecture
1026   and evolution within silicate-rich rocks, such as the conveyor model, may require rethinking in
1027   their application to carbonates. We present the initial ideas of a "dissolving conveyor" and a
1028   "leaky conveyor" as starting points to incorporate carbonate CZ processes. The ability of karst
1029   conduits to transport mobile regolith can lead to decoupling of hillslopes from stream channels,
1030   potentially weakening or eliminating feedback mechanisms that drive landscapes underlain by
1031   silicate-rich rocks toward equilibrium topography and regolith thickness. The fast reaction
1032   kinetics and elevated solubility of carbonate minerals lead to distinct differences in the
1033   relationships between tectonism and carbonate and silicate CZ development, including in the
1034   interactions between base level and the depths of weathering processes. Because of the deep
1035   circulation of meteoric water in karst settings, the lower boundary of the CZ needs to be
1036   expanded, and the definition of the CZ may need modification to include carbonate terrains.

1037   A better understanding of carbonate CZ development may inspire broader conceptual
1038   frameworks that incorporate roles for preferential flow and heterogeneity, which are present to
1039   some extent in all CZ settings. The triple porosity system of matrix, fractures, and karst provides
1040   opportunities to study a spectrum of flow-through timescales and weathering rates and depths in
1041   one setting. Scaling questions are also amplified when there are large contrasts in permeability
1042   that vary with the scale considered. The controlling processes in the conveyor model for
1043   weathering might be better understood by measuring rates in a faster transport system,
1044   particularly under anthropogenic stresses, harking back to the concept of carbonate rocks as a
1045   bellwether. Constraining the transport of gases through the subsurface may enhance our
1046   understanding of the global carbon cycle and how it is affected by biological and geochemical
1047   processes.

1048   Understanding how the CZ evolves along the carbonate-silicate spectrum requires a
1049   broader conceptual framework than we currently have. Many questions arise. What controls the
1050   distribution of CO_2 in the subsurface? How do advective processes influence this distribution?
1051   How do pCO_2, water availability, plant growth, and rock structure interact to determine patterns
1052   of porosity development? Under what conditions do acids other than carbonic acid drive porosity
1053   development? How are feedbacks between biological, hydrological, and geological processes

1054 reflected at the landscape scale? What factors control the partitioning of denudation fluxes
1055 between dissolved vs. solid and subsurface vs. surface? How does this partitioning impact the
1056 dynamics and structure of the CZ? There is a need to integrate knowledge across sites rather than
1057 focusing on the idiosyncratic or distinctive nature of individual sites. In addition to pure
1058 carbonates and pure silicates, there is an entire spectrum of mixtures that lie between these
1059 endmembers. What are the most important parameters along that spectrum that produce
1060 differences in CZ processes and architecture? Answers to these questions will require
1061 transdisciplinary study teams that are integrated into the CZ research community going forward.

1062

1063

1069 **Open Research**

1070 No new data were presented in this review article.

1071

1072 **References**

1073 Adams, C. S., & Swinnerton, A. C. (1937). Solubility of limestone. *Eos, Transactions American*

1074 *Geophysical Union*, *18*(2), 504-508.

1075 Adams, P. N., Opdyke, N. D., & Jaeger, J. M. (2010). Isostatic uplift driven by karstification and

1076 sea-level oscillation: Modeling landscape evolution in north Florida. *Geology*, *38*(6), 531-534.

1077 https://doi.org/10.1130/G30592.1

1078 Allred, K. (2004). Some carbonate erosion rates of southeast Alaska. *Journal of Cave and Karst*

1079 *Studies*, *66*(3), 89-97.

1080 Álvarez Nazario, M. (1972). La herencia lingüística de Canarias en Puerto Rico. *San Juan:*

1081 *Instituto de Cultura Puertorriqueña*, 136-151.

1082   Amundson, R., Richter, D. D., Humphreys, G. S., Jobbágy, E. G., & Gaillardet, J. (2007).

1083   Coupling between biota and earth materials in the critical zone. *Elements*, *3*(5), 327-332.

1084   https://doi.org/10.2113/gselements.3.5.327

1085   Anderson, R. S., Anderson, S. P., & Tucker, G. E. (2013). Rock damage and regolith transport

1086   by frost: An example of climate modulation of the geomorphology of the critical zone. *Earth*

1087   *Surface Processes and Landforms*, *38*(3), 299-316. https://doi.org/10.1002/esp.3330

1088   Anderson, S. P., Dietrich, W. E., & Brimhall Jr, G. H. (2002). Weathering profiles, mass-balance

1089   analysis, and rates of solute loss: Linkages between weathering and erosion in a small, steep

1090   catchment. *Geological Society of America Bulletin*, *114*(9), 1143-1158.

1091   https://doi.org/10.1130/0016-7606(2002)114<1143:WPMBAA>2.0.CO;2

1092   Andre, B. J., & Rajaram, H. (2005). Dissolution of limestone fractures by cooling waters: Early

1093   development of hypogene karst systems. *Water Resources Research*, *41*(1).

1094   Andrews, J. A., & Schlesinger, W. H. (2001). Soil CO_2 dynamics, acidification, and chemical

1095   weathering in a temperate forest with experimental CO_2 enrichment. *Global biogeochemical*

1096   *cycles*, *15*(1), 149-162. https://doi.org/10.1029/2000GB001278

1097   Ashton, K. (1966). The analysis of flow data from karst drainage systems. *Transactions of the*

1098   *Cave Research Group of Great Britain,* 7(2), 161–204.

1099   Atkinson, T. C. (1977a). Diffuse flow and conduit flow in limestone terrain in the Mendip Hills,

1100   Somerset (Great Britain). *Journal of Hydrology, 35*(1-2), 93–110. https://doi.org/10.1016/0022-

1101   1694(77)90079-8

1102   Atkinson, T. C. (1977b). Carbon dioxide in the atmosphere of the unsaturated zone: An

1103   important control of groundwater hardness in limestones. *Journal of Hydrology, 35*(1-2), 111–

1104   123. https://doi.org/10.1016/0022-1694(77)90080-4

1105   Audra, P., Bini, A., Gabrovšek, F., Häuselmann, P., Hobléa, F., Jeannin, P.-Y., Kunaver, J.,

1106   Monbaron, M., Šušteršič, F., Tognini, P., Trimmel, H., Wildberger, A. (2007). Cave and Karst

1107   Evolution in the Alps and Their Relation to Paleoclimate and Paleotopography. *Acta*

1108   *Carsologica, 36*(1), 53-67. https://doi.org/10.3986/ac.v36i1.208

1109   Back, W., Hanshaw, B.B., Herman, J.S., Van Driel, J.N. (1986). Differential dissolution of a

1110   Pleistocene reef in the ground-water mixing zone of coastal Yucatan, Mexico. *Geology, 14*(2),

1111   137–140.

1112   Bajo, P., Borsato, A., Drysdale, R., Hua, Q., Frisia, S., Zanchetta, G., ... & Woodhead, J. (2017).

1113   Stalagmite carbon isotopes and dead carbon proportion (DCP) in a near-closed-system situation:

1114   An interplay between sulphuric and carbonic acid dissolution. *Geochimica et Cosmochimica*

1115   *Acta*, *210*, 208-227.

1116   Baldini, J. U., Bertram, R. A., & Ridley, H. E. (2018). Ground air: A first approximation of the

1117   Earth's second largest reservoir of carbon dioxide gas. *Science of the Total Environment*, 616,

1118   1007-1013.

1119   Balestra, V., & Bellopede, R. (2022). Microplastic pollution in show cave sediments: First

1120   evidence and detection technique. *Environmental Pollution*, *292*, 118261.

1121   Bard, E., Antonioli, F., & Silenzi, S. (2002). Sea-level during the penultimate interglacial period

1122   based on a submerged stalagmite from Argentarola Cave (Italy). *Earth and Planetary Science*

1123   *Letters,* 196(3-4), 135-146.

1124   Beach, T., Luzzadder-Beach, S., Cook, D., Dunning, N., Kennett, D. J., Krause, S., ... & Valdez,

1125   F. (2015). Ancient Maya impacts on the Earth's surface: An Early Anthropocene analog?.

1126   *Quaternary Science Reviews*, *124*, 1-30.

1127   Beaulieu, E., Y. Goddéris, D. Labat, C. Roelandt, D. Calmels, and J. Gaillardet (2011),

1128   Modeling of water-rock interaction in the Mackenzie basin: Competition between

1129   sulfuric and carbonic acids, *Chemical Geology, 289*(1-2), 114-123.

1130   https://doi.org/10.1016/j.chemgeo.2011.07.020

1131   Beerling, D. J., Woodward, F. I., Lomas, M. R., Wills, M. A., Quick, W. P., & Valdes, P. J.

1132   (1998). The influence of Carboniferous palaeoatmospheres on plant function: an experimental

1133   and modelling assessment. *Philosophical Transactions of the Royal Society of London. Series B:*

1134   *Biological Sciences*, *353*(1365), 131-140. https://doi.org/10.1098/rstb.1998.0196

1135   Benavente, J., Vadillo, I., Carrasco, F., Soler, A., Liñán, C., Moral, F. (2010). Air Carbon

1136   Dioxide Contents in the Vadose Zone of a Mediterranean Karst. *Vadose Zone Journal, 9*(1), 126-

1137   136. https://doi.org/10.2136/vzj2009.0027

1138   Berner, R.A. (1992). Weathering, plants, and the long-term carbon cycle. *Geochimica et*

1139   *Cosmochimica Acta, 56*(8), 3225–3231. https://doi.org/10.1016/0016-7037(92)90300-8

1140   Berner, R.A. (1997). The Rise of Plants and Their Effect on Weathering and Atmospheric CO2.

1141   *Science, 276*(5312), 544–546. https://doi.org/10.1126/science.276.5312.544

1142   Billings, S. A., Hirmas, D., Sullivan, P. L., Lehmeier, C. A., Bagchi, S., Min, K. et al. (2018).

1143   Loss of deep roots limits biogenic agents of soil development that are only partially restored by

1144   decades of forest regeneration. *Elementa: Science of the Anthropocene*, *6*(34).

1145   https://doi.org/10.1525/elementa.287

1146   Birk, S., Liedl, R., & Sauter, M. (2006). Karst Spring Responses Examined by Process-Based

1147   Modeling. *Ground Water, 44*(6), 832–836. https://doi.org/10.1111/j.1745-6584.2006.00175.x

1148   Bögli, A. (1964). Mischungskorrosion — Ein Beitrag zum Verkarstungsproblem. *Erdkunde, 18*,

1149   83–92.

1150   Bouchez, J., Gaillardet, J., & von Blanckenburg, F. (2014). Weathering intensity in lowland river

1151   basins: from the Andes to the Amazon mouth. *Procedia earth and planetary science*, *10*, 280-

1152   286.

1153   Brantley, S. L., Eissenstat, D. M., Marshall, J. A., Godsey, S. E., Balogh-Brunstad, Z., Karwan,

1154   D. L., et al. (2017). Reviews and syntheses: on the roles trees play in building and plumbing the

1155   critical zone. *Biogeosciences*, *14*(22), 5115-5142.

1156   Brantley, S.L., Holleran, M.E., Jin, L., & Bazilevskaya, E. (2013). Probing deep weathering in

1157   the Shale Hills Critical Zone Observatory, Pennsylvania (USA): the hypothesis of nested

1158   chemical reaction fronts in the subsurface. *Earth Surf. Process. Landforms, 38*(11), 1280–1298.

1159   https://doi.org/10.1002/esp.3415

1160   Brantley, S.L., Lebedeva, M.I., Balashov, V.N., Singha, K., Sullivan, P.L., & Stinchcomb, G.

1161   (2017a). Toward a conceptual model relating chemical reaction fronts to water flow paths in

1162   hills. *Geomorphology, 277*, 100–117. https://doi.org/10.1016/j.geomorph.2016.09.027

1163   Brantley, S.L., McDowell, W.H., Dietrich, W.E., White, T.S., Kumar, P., Anderson, S.P.,

1164   Chorover, J., Lohse, K.A., Bales, R.C., Richter, D.D., Grant, G., & Gaillardet, J. (2017b).

1165   Designing a network of critical zone observatories to explore the living skin of the terrestrial

1166   Earth. *Earth Surface Dynamics, 5*(4), 841–860. https://doi.org/10.5194/esurf-5-841-2017

1167   Breecker, D. O., Payne, A. E., Quade, J., Banner, J. L., Ball, C. E., Meyer, K. W., & Cowan, B.

1168   D. (2012). The sources and sinks of CO2 in caves under mixed woodland and grassland

1169   vegetation. *Geochimica et Cosmochimica Acta*, *96*, 230-246.

1170   Breithaupt, C. I., Gulley, J. D., Bunge, E. M., Moore, P. J., Kerans, C., Fernandez-Ibanez, F., &

1171   Fullmer, S. M. (2021). A transient, perched aquifer model for banana hole formation: Evidence

1172   from San Salvador Island, Bahamas. *Earth Surface Processes and Landforms, 47*(2), 618-638.

1173   https://doi.org/10.1002/esp.5276

1174   Brookfield, A.E., Macpherson, G.L., & Covington, M.D. (2017). Effects of Changing Meteoric

1175   Precipitation Patterns on Groundwater Temperature in Karst Environments. *Groundwater,*

1176   *552*(2), 227–236. https://doi.org/10.1111/gwat.12456

1177   Brown, A.L., Martin, J.B., Screaton, E.J., Ezell, J.E., Spellman, P., & Gulley, J. (2014). Bank

1178   storage in karst aquifers: The impact of temporary intrusion of river water on carbonate

1179   dissolution and trace metal mobility. *Chemical Geology, 385*, 56–69.

1180   https://doi.org/10.1016/j.chemgeo.2014.06.015

1181   Brown, A.L., Martin, J.B., Kamenov, G.D., Ezell, J.E., Screaton, E.J., Gulley, J., & Spellman, P.

1182   (2019). Trace metal cycling in karst aquifers subject to periodic river water intrusion. *Chemical*

1183   *Geology, 527*, 118773. https://doi.org/10.1016/j.chemgeo.2018.05.020

1184   Brucker, R.W., Hess, J.W., & White, W.B., 1972. Role of Vertical Shafts in the Movement of

1185   Ground Water in Carbonate Aquifers. *Groundwater, 10*(6), 5–13. https://doi.org/10.1111/j.1745-

1186   6584.1972.tb02943.x

1187   Brumm, A., Oktaviana, A. A., Burhan, B., Hakim, B., Lebe, R., Zhao, J. X., ... & Aubert, M.

1188   (2021). Oldest cave art found in Sulawesi. *Science Advances*, *7*(3), eabd4648.

1189   Bufe, A., Hovius, N., Emberson, R., Rugenstein, J. K., Galy, A., Hassenruck-Gudipati, H. J., &

1190   Chang, J. M. (2021). Co-variation of silicate, carbonate and sulfide weathering drives CO2

1191   release with erosion. *Nature Geoscience*, *14*(4), 211-216.

1192   Buhmann, D., & Dreybrodt, W. (1985a). The kinetics of calcite dissolution and precipitation in

1193   geologically relevant situations of karst areas: 1. Open system. *Chemical geology*, 48(1-4), 189-

1194   211.

1195   Buhmann, D., & Dreybrodt, W. (1985b). The kinetics of calcite dissolution and precipitation in

1196   geologically relevant situations of karst areas: 2. Closed system. *Chemical Geology*, 53(1-2),

1197   109-124.

1198   Chen, X., Zhang, Z., Soulsby, C., Cheng, Q., Binley, A., Jiang, R., & Tao, M. (2018).

1199   Characterizing the heterogeneity of karst critical zone and its hydrological function: an integrated

1200   approach. *Hydrological Processes*, 32(19), 2932-2946.

1201   Choquette, P. W., & L. E. Pray (1970), Geologic nomenclature and classification of porosity in

1202   sedimentary carbonates, *American Association of Petroleum Geologists Bulletin, 54*(2), 207-250.

1203   https://doi.org/10.1306/5D25C98B-16C1-11D7-8645000102C1865D

1204   Cohen, M. J., Watts, D. L., Heffernan, J. B., & Osborne, T. Z. (2011). Reciprocal biotic control

1205   on hydrology, nutrient gradients, and landform in the greater everglades. *Critical Reviews in*

1206   *Environmental Science and Technology*, *41*(S1), 395-429.

1207   https://doi.org/10.1080/10643389.2010.531224

1208   Condon, L. E., Markovich, K. H., Kelleher, C. A., McDonnell, J. J., Ferguson, G., & McIntosh,

1209   J. C. (2020). Where is the bottom of a watershed?. *Water Resources Research*, *56*(3),

1210   e2019WR026010. https://doi.org/10.1029/2019WR026010.

1211   Cooper, M.P., & Covington, M.D. (2020). Modeling cave cross-section evolution including

1212   sediment transport and paragenesis. *Earth Surface Processes and Landforms, 45*(11), 2588–

1213   2602. https://doi.org/10.1002/esp.4915

1214   Covington, M. D. (2014). Calcite dissolution under turbulent flow conditions: a remaining

1215   conundrum. *Acta Carsologica*, *43*(1).

1216   Covington, M.D. (2016). The importance of advection for CO_2 dynamics in the karst critical

1217   zone: An approach from dimensional analysis, in: *Geological Society of America Special Papers*

1218   *516: Caves and Karst Across Time*, Geological Society of America, pp. 113–127.

1219   https://doi.org/10.1130/2015.2516(09)

1220   Covington, M. D., Knierim, K. J., Young, H. A., Rodriguez, J., & Gnoza, H. G. (2021). The

1221   impact of ventilation patterns on calcite dissolution rates within karst conduits. *Journal of*

1222   *Hydrology*, *593*, 125824. https://doi.org/10.1016/j.jhydrol.2020.125824

1223   Covington, M. D., Luhmann, A. J., Wicks, C. M., & Saar, M. O. (2012). Process length scales

1224   and longitudinal damping in karst conduits. *Journal of Geophysical Research: Earth Surface*,

1225   *117*(F1). https://doi.org/10.1029/2011JF002212

1226   Covington, M. D., & Perne, M. (2015). Consider a cylindrical cave: A physicist's view of cave

1227   and karst science. *Acta Carsologica*, *44*(3).

1228   Covington, M.D., Prelovšek, M., & Gabrovšek, F. (2013). Influence of CO2 dynamics on the

1229   longitudinal variation of incision rates in soluble bedrock channels: feedback mechanisms,

1230   *Geomorphology, 186*, 85-95, https://doi:10.1016/j.geomorph.2012.12.025.

1231   Covington, M.D., Vaughn, K.A. (2019). Carbon dioxide and dissolution rate dynamics within a

1232   karst underflow-overflow system, Savoy Experimental Watershed, Arkansas, USA. *Chemical*

1233   *Geology*, *527*, 118689. https://doi.org/10.1016/j.chemgeo.2018.03.009

1234   Culver, D.C., Pipan, T., 2013. Subterranean Ecosystems, in: Levin, S.A. (Ed), *Encyclopedia of*

1235   *Biodiversity*. Academic Press, pp. 49–62. https://doi.org/10.1016/B978-0-12-384719-5.00224-0

1236   Cvijić, J. (1924). Types morphologiques des terrains calcaires. *Bulletin of the Serbian*

1237   *geographical society*, *10*(1), 1-7.

1238   D'Angeli, I. M., Parise, M., Vattano, M., Madonia, G., Galdenzi, S., & De Waele, J. (2019).

1239   Sulfuric acid caves of Italy: A review. *Geomorphology*, *333*, 105-122.

1240   https://doi.org/10.1016/j.geomorph.2019.02.025.

1241   Dammeyer, H. C., Schwinning, S., Schwartz, B. F., & Moore, G. W. (2016). Effects of juniper

1242   removal and rainfall variation on tree transpiration in a semi-arid karst: Evidence of complex

1243   water storage dynamics. *Hydrological Processes*, *30*, 4568–4581.

1244   Davis, D.G., 1980. Cave development in the Guadalupe Mountains: a critical review of recent

1245   hypotheses. *NSS Bulletin, 42*, 42–48.

1246   Davis, D. M., & Engelder, T. (1985). The role of salt in fold-and-thrust belts. *Tectonophysics*,

1247   *119*(1-4), 67-88.

1248   Day, C. C., von Strandmann, P. A. P., & Mason, A. J. (2021). Lithium isotopes and partition

1249   coefficients in inorganic carbonates: Proxy calibration for weathering reconstruction.

1250   *Geochimica et Cosmochimica Acta*, *305*, 243-262.

1251   Dellinger, M., Bouchez, J., Gaillardet, J., Faure, L., & Moureau, J. (2017). Tracing weathering

1252   regimes using the lithium isotope composition of detrital sediments. *Geology*, *45*(5), 411-414.

1253   Deng, Y., Jiang, Z., & Qin, X. (2012). Water source partitioning among trees growing on

1254   carbonate rock in a subtropical region of Guangxi, China. *Environmental Earth Sciences, 66*,

1255   635–640.

1256   Deuerling, K. M., Martin, J. B., Martin, E. E., Abermann, J., Myreng, S. M., Petersen, D., &

1257   Rennermalm, Å. K. (2019). Chemical weathering across the western foreland of the Greenland

1258   Ice Sheet. *Geochimica et Cosmochimica Acta*, *245*, 426-440.

1259   Dominguez-Cristobal, C. (1989). *La Toponomia del Ciales decimonónico (Vol. 1)*. Instituto

1260   Internacional de Dasonomía Tropical, San Juan.

1261   Dominguez-Cristobal, C. (1992). *La Toponomia del Ciales decimonónico (Vol. 2)*. Instituto

1262   Internacional de Dasonomía Tropical, San Juan.

1263   Cristóbal, C. M. D. (2007). Leyendas indigenas de la zona del carso norteño de Puerto Rico: el

1264   caliche de Ciales. *Acta Cientifica*, *21*(1-3), 81-83.

1265   Dong, X., Cohen, M. J., Martin, J. B., McLaughlin, D. L., Murray, A. B., Ward, N. D., et al.

1266   (2019a). Ecohydrologic processes and soil thickness feedbacks control limestone-weathering

1267   rates in a karst landscape. *Chemical Geology*, *527*, 118774.

1268   https://doi.org/10.1016/j.chemgeo.2018.05.021

1269   Dong, X., Murray, A.B., & Heffernan, J.B. (2019b). Ecohydrologic feedbacks controlling sizes

1270   of cypress wetlands in a patterned karst landscape. *Earth Surface Processes and Landforms, 44,*

1271   1178–1191. https://doi.org/10.1002/esp.4564

1272   Drake, J. J. (1980). The effect of soil activity on the chemistry of carbonate groundwaters. *Water*

1273   *Resources Research*, *16*(2), 381-386. https://doi.org/10.1029/WR016i002p00381

1274   Drever, J.I. (1994). The effect of land plants on weathering rates of silicate minerals. *Geochimica*

1275   *et Cosmochimica Acta, 58*, 2325–2332. https://doi.org/10.1016/0016-7037(94)90013-2

1276   Dreybrodt, W. (1990). The Role of Dissolution Kinetics in the Development of Karst Aquifers in

1277   Limestone: A Model Simulation of Karst Evolution. *The Journal of Geology, 98*, 639–655.

1278   Dreybrodt, W. (1996). Principles of Early Development of Karst Conduits Under Natural and

1279   Man-Made Conditions Revealed by Mathematical Analysis of Numerical Models. *Water Resour.*

1280   *Res., 32*, 2923–2935. https://doi.org/10.1029/96WR01332

1281   Druhan, J. L., Lawrence, C. R., Covey, A. K., Giannetta, M. G., & Oster, J. L. (2021). A reactive

1282   transport approach to modeling cave seepage water chemistry I: Carbon isotope transformations.

1283   *Geochimica et Cosmochimica Acta*, 311, 374-400.

1284   Dublyansky, Y. V. (1995). Speleogenetic history of the Hungarian hydrothermal karst.

1285   *Environmental Geology*, *25*(1), 24-35.

1286   C. Dubois, Y. Quinif, J.-M. Baele, L. Barriquand, A. Bini, L. Bruxelles, G. Dandurand, C.

1287   Havron, O. Kaufmann, B., Lans, R. Maire, J. Martin, J. Rodet, M.D., et al. (2014). The process

1288   of ghost-rock karstification and its role in the formation of cave systems, *Earth Sci. Rev.*, 131,

1289   166-148.

1290   Engel, A. S., L. A. Stern, & P. C. Bennett (2004), Microbial contributions to cave formation:

1291   New insights into sulfuric acid speleogenesis, *Geology, 32*(5), 369-372.

1292   Egemeier, S.J. (1987). A theory for the origin of Carlsbad Caverns. *NSS Bulletin. 49*, 73–76.

1293   Egemeier, S. J. (1988), Cavern development by thermal water, *NSS Bulletin, 43*, 31-51.

1294   Ellsworth, P. Z., & Sternberg, L. S. L. (2015). Seasonal water use by deciduous and evergreen

1295   woody species in a scrub community is based on water availability and root distribution.

1296   *Ecohydrology, 8*, 538–551.

1297   Erlanger, E. D., Rugenstein, J. K. C., Bufe, A., Picotti, V., & Willett, S. D. (2021). Controls on

1298   Physical and Chemical Denudation in a Mixed Carbonate-Siliciclastic Orogen. *Journal of*

1299   *Geophysical Research: Earth Surface*, *126*(8), e2021JF006064.

1300   Estrada-Medina, H., Graham, R. C., Allen, M. F., Jiménez-Osornio, J. J., & Robles-Casolco, S.

1301   (2013). The importance of limestone bedrock and dissolution karst features on tree root

1302   distribution in northern Yucatán, México. *Plant and soil*, *362*(1), 37-50.

1303   Ewers, O.R. (1982). *Cavern development in the dimensions of length and breadth* (Doctoral

1304   dissertation). Hamilton, Canada: McMaster University.

1305   Faimon, J., Lang, M., Geršl, M., Sracek, O., & Bábek, O. (2020). The "breathing spots" in karst

1306   areas—the sites of advective exchange of gases between soils and adjacent underground cavities.

1307   *Theoretical and Applied Climatology*, *142*(1), 85-101. https://doi.org/10.1007/s00704-020-

1308   03280-7

1309   Fairchild, I. J., Smith, C. L., Baker, A., Fuller, L., Spötl, C., Mattey, D., & McDermott, F.

1310   (2006). Modification and preservation of environmental signals in speleothems. *Earth-Science*

1311   *Reviews*, *75*(1-4), 105-153. https://doi.org/10.1016/j.earscirev.2005.08.003

1312   Farrant, A.R., & Smart, P.L. (2011). Role of sediment in speleogenesis; sedimentation and

1313   paragenesis. *Geomorphology, 134*, 79–93. https://doi.org/10.1016/j.geomorph.2011.06.006

1314   Filipponi, M., Jeannin, P.-Y., & Tacher, L. (2009). Evidence of inception horizons in karst

1315   conduit networks. *Geomorphology, 106*, 86–99. https://doi.org/10.1016/j.geomorph.2008.09.010

1316   Fischedick, M., Roy, J., Acquaye, A., Allwood, J., Ceron, J. P., Geng, Y., et al. (2014). Industry

1317   In: *Climate Change 2014: Mitigation of Climate Change. Contribution of Working Group III to*

1318   *the Fifth Assessment Report of the Intergovernmental Panel on Climate Change.* Technical

1319   Report. Cambridge University Press, Cambridge, United Kingdom.

1320   Flint, M. K., Martin, J. B., Summerall, T. I., Barry-Sosa, A., & Christner, B. C. (2021). Nitrous

1321   oxide processing in carbonate karst aquifers. *Journal of hydrology*, *594*, 125936.

1322   Florea, L.J., & Vacher, H.L. (2006). Springflow Hydrographs: Eogenetic vs. Telogenetic Karst.

1323   *Ground Water, 44*, 352–361. https://doi.org/10.1111/j.1745-6584.2005.00158.x

1324   Florea, L.J., Vacher, H.L., Donahue, B., & Naar, D. (2007). Quaternary cave levels in peninsular

1325   Florida. *Quaternary Science Reviews*, *26*, 1344–1361.

1326   https://doi.org/10.1016/j.quascirev.2007.02.011

1327   Fohlmeister, J., Scholz, D., Kromer, B., & Mangini, A. (2011). Modelling carbon isotopes of

1328   carbonates in cave drip water. *Geochimica et Cosmochimica Acta*, 75(18), 5219-5228.

1329   Fohlmeister, J., Voarintsoa, N.R.G., Lechleitner, F.A., Boyd, M., Brandtstätter, S., Jacobson,

1330   M.J., & Oster, J.L. (2020). Main controls on the stable carbon isotope composition of

1331   speleothems. *Geochimica et Cosmochimica Acta, 279*, 67–87.

1332   https://doi.org/10.1016/j.gca.2020.03.042

1333   Ford, D. C. (1971). Alpine Karst in the Mt. Castleguard-Columbia icefield area, Canadian Rocky

1334   Mountains. *Arctic and Alpine Research*, *3*(3), 239-252.

1335   Ford, D. C., Lauritzen, S. E., & Ewers, R. O. (2000). Modeling of initiation and propagation of

1336   single conduits and networks. *Speleogenesis: Evolution of Karst Aquifers. Huntsville, Ala.,*

1337   *National Speleological Society*, 175-183.

1338   Ford, D., & Williams, P.D. (2007). *Karst hydrogeology and geomorphology*. John Wiley &

1339   Sons.

1340 Frumkin, A., 2013. Salt karst. In: Shroder, J. (Editor in Chief), Frumkin, A. (Ed.), *Treatise on*

1341 *Geomorphology, Karst Geomorphology*. Academic Press, San Diego, CA, 407-424.

1342 Fu, T., Chen, H., Fu, Z., & Wang, K. (2016). Surface soil water content and its controlling

1343 factors in a small karst catchment. *Environmental Earth Sciences, 75*, 1406.

1344 Gabet, E. J., & Mudd, S. M. (2009). A theoretical model coupling chemical weathering rates

1345 with denudation rates. *Geology*, *37*(2), 151-154.

1346 Gabrovšek, F. (2009). On concepts and methods for the estimation of dissolutional denudation

1347 rates in karst areas. *Geomorphology, 106*, 9–14. https://doi.org/10.1016/j.geomorph.2008.09.008

1348 Gabrovšek, F., & Dreybrodt, W. (2001). A model of the early evolution of karst aquifers in

1349 limestone in the dimensions of length and depth. *Journal of Hydrology, 240*, 206–224.

1350 https://doi.org/10.1016/S0022-1694(00)00323-1

1351 Gabrovšek, F., Häuselmann, P., & Audra, P. (2014). 'Looping caves' versus 'water table caves':

1352 The role of base-level changes and recharge variations in cave development. *Geomorphology,*

1353 *204*, 683–691. https://doi.org/10.1016/j.geomorph.2013.09.016

1354 Gaillardet, J., Braud, I., Hankard, F., Anquetin, S., Bour, O., Dorfliger, N., ... & Zitouna, R.

1355 (2018). OZCAR: The French network of critical zone observatories. *Vadose Zone Journal*, 17(1),

1356 1-24.

1357 Gaillardet, J., Calmels, D., Romero-Mujalli, G., Zakharova, E., & Hartmann, J. (2019). Global

1358 climate control on carbonate weathering intensity. *Chemical Geology*, *527*, 118762.

1359 https://doi.org/10.1016/j.chemgeo.2018.05.009

1360 Galloway, J. N. (1998). The global nitrogen cycle: changes and consequences. *Environmental*

1361 *pollution*, *102*(1), 15-24.

1362 Galloway, J. N., Townsend, A. R., Erisman, J. W., Bekunda, M., Cai, Z., Freney, J. R., et al.

1363 (2008). Transformation of the nitrogen cycle: recent trends, questions, and potential solutions.

1364 *Science*, *320*(5878), 889-892.

1365 Gandois, L., A.-S. Perrin, & A. Probst (2011). Impact of nitrogenous fertiliser-induced proton

1366 release on cultivated soils with contrasting carbonate contents: a column experiment.

1367 *Geochimica et cosmochimica acta, 75*(5): 1185-1198.

1368 Garcia, A. A., Semken, S., & Brandt, E. (2020). The Construction of Cultural Consensus Models

1369 to Characterize Ethnogeological Knowledge. *Geoheritage, 12*(3), 59.

1370 https://doi.org/10.1007/s12371-020-00480-5

1371 Gary, M. O., & Sharp, J. M. (2006). Volcanogenic karstification of Sistema Zacatón, Mexico.

1372 *Special Papers-Geological Society of America*, *404*, 79.

1373 Geekiyanage, N., Goodale, U. M., Cao, K., & Kitajima, K. (2019). Plant ecology of tropical and

1374 subtropical karst ecosystems. *Biotropica*, *51*(5), 626-640.

1375 Goldscheider, N., Chen, Z., Auler, A. S., Bakalowicz, M., Broda, S., Drew, D., et al. (2020).

1376 Global distribution of carbonate rocks and karst water resources. *Hydrogeology Journal*, *28*(5),

1377 1661-1677. https://doi.org/10.1007/s10040-020-02139-5

1378 Gombert, P. (2002). Role of karstic dissolution in global carbon cycle. *Global and Planetary*

1379 *Change, 33*, 177–184. https://doi.org/10.1016/S0921-8181(02)00069-3

1380 Gonzalez, B. C., Iliffe, T. M., Macalady, J. L., Schaperdoth, I., & Kakuk, B. (2011). Microbial

1381 hotspots in anchialine blue holes: initial discoveries from the Bahamas. *Hydrobiologia*, *677*(1),

1382 149-156.

1383 Granger, D.E., Fabel, D., & Palmer, A.N. (2001). Pliocene-Pleistocene incision of the Green

1384 River, Kentucky, determined from radioactive decay of cosmogenic 26Al and 10Be in Mammoth

1385 Cave sediments. *Geological Society of America Bulletin, 113*, 825–836.

Green, S.M., Dungait, J.A.J., Tu, C., Buss, H.L., Sanderson, N., Hawkes, S.J., et al. (2019). Soil functions and ecosystem services research in the Chinese karst Critical Zone. *Chemical Geology, 527*, 119107. https://doi.org/10.1016/j.chemgeo.2019.03.018

Griffiths, M. L., Fohlmeister, J., Drysdale, R. N., Hua, Q., Johnson, K. R., Hellstrom, J. C., ... & Zhao, J. X. (2012). Hydrological control of the dead carbon fraction in a Holocene tropical speleothem. *Quaternary Geochronology*, *14*, 81-93.

Groves, C., & Hendrikson, M. (2011). From sink to resurgence: the buffering capacity of a cave system in the Tongass National Forest, USA. *Acta Carsologica, 391*.

Groves, C.G., & Howard, A.D. (1994). Minimum hydrochemical conditions allowing limestone cave development. *Water Resour. Res., 30*, 607–615. https://doi.org/10.1029/93WR02945

Groves, C., & Meiman, J. (2005). Weathering, geomorphic work, and karst landscape evolution in the Cave City groundwater basin, Mammoth Cave, Kentucky. *Geomorphology, 67*, 115–126. https://doi.org/10.1016/j.geomorph.2004.07.008

Gulley, J.D., Martin, J.B., & Brown, A. (2016). Organic carbon inputs, common ions and degassing: rethinking mixing dissolution in coastal eogenetic carbonate aquifers: Rethinking Mixing Dissolution in Coastal Eogenetic Carbonate Aquifers. *Earth Surf. Process. Landforms, 41*, 2098–2110. https://doi.org/10.1002/esp.3975

Gulley, J.D., Martin, J.B., Moore, P.J., Brown, A., Spellman, P.D., & Ezell, J. (2015). Heterogeneous distributions of CO_2 may be more important for dissolution and karstification in coastal eogenetic limestone than mixing dissolution. *Earth Surf. Process. Landforms, 40*, 1057–1071. https://doi.org/10.1002/esp.3705

Gulley, J.D., Martin, J.B., Moore, P.J., & Murphy, J. (2013). Formation of phreatic caves in an eogenetic karst aquifer by CO_2 enrichment at lower water tables and subsequent flooding by sea level rise. *Earth Surf. Process. Landforms, 38*, 1210–1224. https://doi.org/10.1002/esp.3358

1410   Gulley, J., Martin, J., & Moore, P. (2014). Vadose CO2 gas drives dissolution at water tables in

1411   eogenetic karst aquifers more than mixing dissolution. *Earth Surf. Process. Landforms, 39*,

1412   1833–1846. https://doi.org/10.1002/esp.3571

1413   Gulley, J., Martin, J.B., Screaton, E.J., & Moore, P.J. (2011). River reversals into karst springs:

1414   A model for cave enlargement in eogenetic karst aquifers. *Geological Society of America*

1415   *Bulletin, 123*, 457–467. https://doi.org/10.1130/B30254.1

1416   Gulley, J., Martin, J., Spellman, P., Moore, P., & Screaton, E. (2013). Dissolution in a variably

1417   confined carbonate platform: effects of allogenic runoff, hydraulic damming of groundwater

1418   inputs, and surface-groundwater exchange at the basin scale. *Earth Surf. Process. Landforms*, *38*,

1419   1700–1713. https://doi.org/10.1002/esp.3411

1420   Gunn, J. (1981). Limestone solution rates and processes in the Waitomo district, New Zealand.

1421   *Earth Surface Processes and Landforms*, *6*(5), 427-445.

1422   Gutiérrez, F., Parise, M., De Waele, J., & Jourde, H. (2014). A review on natural and human-

1423   induced geohazards and impacts in karst. *Earth-Science Reviews*, *138*, 61-88.

1424   Haas, S., De Beer, D., Klatt, J. M., Fink, A., Rench, R. M., Hamilton, T. L., et al. (2018). Low-

1425   light anoxygenic photosynthesis and Fe-S-biogeochemistry in a microbial mat. *Frontiers in*

1426   *Microbiology*, *9*, 858.

1427   Halihan, T., Sharp, J. M., & Mace, R. E. (2000). Flow in the San Antonio segment of the

1428   Edwards aquifer: matrix, fractures, or conduits?. In Sasowsky, I. D., & Wicks, C. M. (Eds),

1429   *Groundwater flow and contaminant transport in carbonate aquifers.* CRC Press. (pp. 129-146).

1430   Hanna, R. B., & Rajaram, H. (1998). Influence of aperture variability on dissolutional growth of

1431   fissures in karst formations. *Water Resources Research*, *34*(11), 2843-2853.

1432   https://doi.org/10.1029/98WR01528

1433   Hartmann, A., Goldscheider, N., Wagener, T., Lange, J., & Weiler, M. (2014). Karst water

1434   resources in a changing world: Review of hydrological modeling approaches. *Reviews of*

1435   *Geophysics*, *52*(3), 218-242.

1436   Hartmann, A., Gleeson, T., Wada, Y., & Wagener, T. (2017). Enhanced groundwater recharge

1437   rates and altered recharge sensitivity to climate variability through subsurface heterogeneity.

1438   *Proceedings of the National Academy of Sciences*, *114*(11), 2842-2847.

1439   Hartmann, A., Jasechko, S., Gleeson, T., Wada, Y., Andreo, B., Barberá, J. A., ... & Wagener, T.

1440   (2021). Risk of groundwater contamination widely underestimated because of fast flow into

1441   aquifers. *Proceedings of the National Academy of Sciences*, *118*(20), e2024492118.

1442   Hartmann, J., & Moosdorf, N. (2012). The new global lithological map database GLiM: A

1443   representation of rock properties at the Earth surface. *Geochemistry, Geophysics, Geosystems,*

1444   *13*. https://doi.org/10.1029/2012GC004370

1445   Häuselmann, P., & Tognini, P. (2005). Kaltbach cave (Siebenhengste, Switzerland): Phantom of

1446   the sandstone? *Acta carsologica, 34*.

1447   Heimsath, A.M., Chadwick, O.A., Roering, J.J., & Levick, S.R. (2020). Quantifying erosional

1448   equilibrium across a slowly eroding, soil mantled landscape. *Earth Surface Processes and*

1449   *Landforms, 45*, 499–510. https://doi.org/10.1002/esp.4725

1450   Heimsath, A.M., Dietrich, W.E., Nishiizumi, K., & Finkel, R.C. (1997). The soil production

1451   function and landscape equilibrium. *Nature, 388*, 358–361. https://doi.org/10.1038/41056

1452   Hendy, C. H. (1971). The isotopic geochemistry of speleothems—I. The calculation of the

1453   effects of different modes of formation on the isotopic composition of speleothems and their

1454   applicability as palaeoclimatic indicators. *Geochimica et cosmochimica Acta*, 35(8), 801-824.

1455   Henry, P. J. (1978). *Mechanique lineaire de la rupture applique a l'etude de la fissuration et de*

1456   *la fracture de roches calcaires,* (Doctoral dissertation). Lille, France: Lille University of Science

1457   and Technology.

1458   Herman, E.K., Toran, L., & White, W.B. (2012). Clastic sediment transport and storage in

1459   fluviokarst aquifers: an essential component of karst hydrogeology. *Carbonates Evaporites, 27*,

1460   211–241. https://doi.org/10.1007/s13146-012-0112-7

1461   Hill, C.A. (1990). Sulfuric Acid Speleogenesis of Carlsbad Cavern and Its Relationship to

1462   Hydrocarbons, Delaware Basin, New Mexico and Texas. *AAPG Bulletin, 74*, 1685–1694.

1463   https://doi.org/10.1306/0C9B2565-1710-11D7-8645000102C1865D

1464   Hilley, G.E., Chamberlain, C.P., Moon, S., Porder, S., & Willett, S.D. (2010). Competition

1465   between erosion and reaction kinetics in controlling silicate-weathering rates. *Earth and*

1466   *Planetary Science Letters, 293*, 191–199. https://doi.org/10.1016/j.epsl.2010.01.008

1467   Houillon, N., Lastennet, R., Denis, A., Malaurent, P., Minvielle, S., & Peyraube, N. (2017).

1468   Assessing cave internal aerology in understanding carbon dioxide (CO2) dynamics: implications

1469   on calcite mass variation on the wall of Lascaux Cave (France). *Environ Earth Sci, 76*, 170.

1470   https://doi.org/10.1007/s12665-017-6498-8

1471   Hu, M., & Hueckel, T. (2019). Modeling of subcritical cracking in acidized carbonate rocks via

1472   coupled chemo-elasticity. *Geomechanics for Energy and the Environment*, *19*, 100114.

1473   Huang, Y., Zhao, P., Zhang, Z., Li, X., He, C., & Zhang, R. (2009). Transpiration of

1474   Cyclobalanopsis glauca (syn. Quercus glauca) stand measured by sap-flow method in a karst

1475   rocky terrain during dry season. *Ecological Research, 24,* 791–801.

1476   Irwin, J. G., & Williams, M. L. (1988). Acid rain: chemistry and transport. *Environmental*

1477   *Pollution, 50*(1-2), 29-59.

1478   Jackson, R.B., Canadell, J., Ehleringer, J.R., Mooney, H.A., Sala, O.E., & Schulze, E.D. (1996).

1479   A global analysis of root distributions for terrestrial biomes. *Oecologia, 108*, 389–411.

1480   https://doi.org/10.1007/BF00333714

1481   Jagnow, D.H., Hill, C.A., Davis, D.G., DuChene, H.R., Cunningham, K.I., Northup, D.E. et al.

1482   (2000). History of the sulfuric acid theory of speleogenesis in the Guadalupe Mountains, New

1483   Mexico. *Journal of Cave and Karst Studies, 62,* 54–59.

1484   Jiang, Z., Lian, Y., & Qin, X. (2014). Rocky desertification in Southwest China: impacts, causes,

1485   and restoration. *Earth-Science Reviews*, *132*, 1-12.

1486   https://doi.org/10.1016/j.earscirev.2014.01.005.

1487   Jobbágy, E.G., & Jackson, R.B. (2000). The Vertical Distribution of Soil Organic Carbon and Its

1488   Relation to Climate and Vegetation. *Ecological Applications, 10*, 423–436.

1489   https://doi.org/10.1890/1051-0761(2000)010[0423:TVDOSO]2.0.CO;2

1490   Jones, D. S., Polerecky, L., Galdenzi, S., Dempsey, B. A. & Macalady, J. L. (2015). Fate of

1491   sulfide in the Frasassi cave system and implications for sulfuric acid speleogenesis. *Chemical*

1492   *Geology, 410*, 21–27.

1493   Jourde, H., Massei, N., Mazzilli, N., Binet, S., Batiot-Guilhe, C., Labat, D., ... & Wang, X.

1494   (2018). SNO KARST: A French network of observatories for the multidisciplinary study of

1495   critical zone processes in karst watersheds and aquifers. *Vadose Zone Journal*, 17(1), 1-18.

1496   Khadka, M.B., Martin, J.B., & Jin, J. (2014). Transport of dissolved carbon and CO_2 degassing

1497   from a river system in a mixed silicate and carbonate catchment. *Journal of Hydrology, 513*,

1498   391–402.

1499   Kim, H., Stinchcomb, G., & Brantley, S.L. (2017). Feedbacks among O_2 and CO_2 in deep soil

1500   gas, oxidation of ferrous minerals, and fractures: A hypothesis for steady-state regolith thickness.

1501   *Earth and Planetary Science Letters, 460*, 29–40. https://doi.org/10.1016/j.epsl.2016.12.003

1502   Király, L. (1975). Rapport sur l'état actuel des connaissances dans le domaine des caractères

1503   physiques des roches karstiques. *Hydrogeology of karstic terrains (Hydrogéologie des terrains*

1504   *karstiques) International Union of geological sciences, 3,* 53–67.

1505   Klappa, C. F. (1980). Brecciation textures and tepee structures in Quaternary calcrete (caliche)
1506   profiles from eastern Spain: the plant factor in their formation. *Geological Journal*, *15*(2), 81-89.
1507   Klimchouk, A. (2004). Towards defining, delimiting and classifying epikarst: Its origin,

1508   processes and variants of geomorphic evolution. *Speleogenesis and Evolution of Karst Aquifers,*

1509   *2*, 1–13.

1510   Klimchouk, A. B. (2007). Hypogene speleogenesis: Hydrogeological and Morphogenetic

1511   Perspective. NCKRI-Special Paper 1.

1512   Klimchouk, A., Palmer, A. N., De Waele, J., Auler, A. S., & Audra, P. (Eds.). (2017). *Hypogene*

1513   *karst regions and caves of the world*. Springer.

1514   Klimchouk, A. (2019). Krubera (Voronja) Cave, in: Encyclopedia of Caves. Elsevier, pp. 627–

1515   634.

1516   Klimchouk, A., Forti, P., & Cooper, A. (1996). Gypsum karst of the World: a brief overview.

1517   *International Journal of Speleology, 25*, 3-4, 159-181.

1518   Klimchouk, A., Evans, D., Milanovic, S., Bittencourt, C., Sanchez, M., & Aguirre, F. C. (2023).

1519   Hypogene speleogenesis related to porphyry magmatic intrusions and its influence on subsequent

1520   karst evolution in the Peruvian high Andes. *Geomorphology*, *420*, 108488.

1521   Kogovšek, J., & Petrič, M. (2012). Characterization of the vadose flow and its influence on the

1522   functioning of karst springs: Case study of the karst system near Postojna, Slovenia. *Acta*

1523   *carsologica, 41.*

1524   Kowalczk, A.J., & Froelich, P.N. (2010). Cave air ventilation and CO2 outgassing by radon-222

1525   modeling: How fast do caves breathe? *Earth and Planetary Science Letters, 289*, 209–219.

1526   https://doi.org/10.1016/j.epsl.2009.11.010

1527   Krklec, K., Braucher, R., Perica, D., & Domínguez-Villar, D. (2022). Long-term denudation rate

1528   of karstic North Dalmatian Plain (Croatia) calculated from 36Cl cosmogenic nuclides.

1529   *Geomorphology*, *413*, 108358.

1530   Kůrková, I., Bruthans, J., Balák, F., Slavík, M., Schweigstillová, J., Bruthansová, J., et al. (2019).

1531   Factors controlling evolution of karst conduits in sandy limestone and calcareous sandstone

1532   (Turnov area, Czech Republic). *Journal of Hydrology, 574*, 1062–1073.

1533   https://doi.org/10.1016/j.jhydrol.2019.05.013

1534   Lang, M., Faimon, J., Godissart, J., & Ek, C. (2017). Carbon dioxide seasonality in dynamically

1535   ventilated caves: the role of advective fluxes. *Theor Appl Climatol, 129,* 1355–1372.

1536   https://doi.org/10.1007/s00704-016-1858-y

1537   Larson, E.B., & Mylroie, J.E. (2018). Diffuse Versus Conduit Flow in Coastal Karst Aquifers:

1538   The Consequences of Island Area and Perimeter Relationships. *Geosciences, 8*, 268.

1539   https://doi.org/10.3390/geosciences8070268

1540   Lauritzen, S. E. (1990). Autogenic and allogenic denudation in carbonate karst by the multiple

1541   basin method: an example from Svartisen, north Norway. *Earth Surface Processes and*

1542   *Landforms*, *15*(2), 157-167.

1543   Lebedeva, M.I., Fletcher, R.C., Brantley, S.L. (2010). A mathematical model for steady-state

1544   regolith production at constant erosion rate. *Earth Surf. Process. Landforms, 35*, 508–524.

1545   https://doi.org/10.1002/esp.1954

1546   Lechleitner, F. A., Day, C. C., Kost, O., Wilhelm, M., Haghipour, N., Henderson, G. M., & Stoll,

1547   H. M. (2021). Stalagmite carbon isotopes suggest deglacial increase in soil respiration in western

1548   Europe driven by temperature change. *Climate of the Past*, *17*(5), 1903-1918.

1549   Lehmann, H. (1936). Morphologische Studien auf Java: Geog. Abhandlungen, III, Stuttgart

1550   1954, 144.

1551 Liu, Z., Groves, C., Yuan, D., Meiman, J., Jiang, G., He, S., et al. (2004). Hydrochemical

1552 variations during flood pulses in the south-west China peak cluster karst: impacts of CaCO3–

1553 H2O–CO2 interactions. *Hydrol. Process., 18*, 2423–2437. https://doi.org/10.1002/hyp.1472

1554 Liu, Z., Li, Q., Sun, H., & Wang, J. (2007). Seasonal, diurnal and storm-scale hydrochemical

1555 variations of typical epikarst springs in subtropical karst areas of SW China: Soil CO2 and

1556 dilution effects. *Journal of Hydrology, 337*, 207–223.

1557 https://doi.org/10.1016/j.jhydrol.2007.01.034

1558 Long, K. E., Schneider, L., Connor, S. E., Shulmeister, N., Finn, J., Roberts, G. L., ... & Haberle,

1559 S. G. (2021). Human impacts and Anthropocene environmental change at Lake Kutubu, a

1560 Ramsar wetland in Papua New Guinea. *Proceedings of the National Academy of Sciences*,

1561 *118*(40), e2022216118.

1562 Lowe, D.J., & Gunn, J. (1997). Carbonate speleogenesis: An inception horizon hypothesis. *Acta*

1563 *Carsologica, 38*, 457–488.

1564 Lucha, P., Gutiérrez, F., Galve, J. P., & Guerrero, J. (2012). Geomorphic and stratigraphic

1565 evidence of incision-induced halokinetic uplift and dissolution subsidence in transverse

1566 drainages crossing the evaporite-cored Barbastro–Balaguer Anticline (Ebro Basin, NE Spain).

1567 *Geomorphology*, *171*, 154-172. https://doi.org/10.1016/j.geomorph.2012.05.015.

1568 Macpherson, G.L., & Sullivan, P.L. (2019a). Watershed-scale chemical weathering in a

1569 merokarst terrain, northeastern Kansas, USA. *Chemical Geology*, *527*, 118988.

1570 https://doi.org/10.1016/j.chemgeo.2018.12.001

1571 Macpherson, G.L., & Sullivan, P.L. (2019b). Dust, impure calcite, and phytoliths: Modeled

1572 alternative sources of chemical weathering solutes in shallow groundwater. *Chemical Geology,*

1573 *527*, 118871. https://doi.org/10.1016/j.chemgeo.2018.08.007

Martin, J.B. (2017). Carbonate minerals in the global carbon cycle. *Chemical Geology, 449*, 58–72. https://doi.org/10.1016/j.chemgeo.2016.11.029

Martin, J.B., & Dean, R.W. (1999). Temperature as a natural tracer of short residence times for groundwater in karst aquifers. *Karst Modeling. Karst Waters Institute Special Publication,* 5, 236–242.

Martin, J.B., & Dean, R.W. (2001). Exchange of water between conduits and matrix in the Floridan aquifer. *Chemical Geology, 179*, 145–165. https://doi.org/10.1016/S0009-2541(01)00320-5

Martin, J. B., Gulley, J., & Spellman, P. (2012). Tidal pumping of water between Bahamian blue holes, aquifers, and the ocean. *Journal of Hydrology*, *416*, 28-38.

Martin, J. B., deGrammont, P. C., Covington, M. D., & Toran, L. (2021). A new focus on the neglected carbonate critical zone. EOS, 102.

Mattey, D.P., Atkinson, T.C., Barker, J.A., Fisher, R., Latin, J.-P., Durrell, R., et al. (2016). Carbon dioxide, ground air and carbon cycling in Gibraltar karst. *Geochimica et Cosmochimica Acta, 184*, 88–113. https://doi.org/10.1016/j.gca.2016.01.041

Mijares, A. S., Détroit, F., Piper, P., Grün, R., Bellwood, P., Aubert, M., ... & Dizon, E. (2010). New evidence for a 67,000-year-old human presence at Callao Cave, Luzon, Philippines. *Journal of human evolution*, *59*(1), 123-132.

Milanolo, S., & Gabrovšek, F. (2009). Analysis of Carbon Dioxide Variations in the Atmosphere of Srednja Bijambarska Cave, Bosnia and Herzegovina. *Boundary-Layer Meteorol, 131*, 479–493. https://doi.org/10.1007/s10546-009-9375-5

Miorandi, R., Borsato, A., Frisia, S., Fairchild, I.J., & Richter, D.K. (2010). Epikarst hydrology and implications for stalagmite capture of climate changes at Grotta di Ernesto (NE Italy): results from long-term monitoring. *Hydrol. Process., 24,* 3101–3114. https://doi.org/10.1002/hyp.7744

1598   Monroe, W.H. (1976). The karst landforms of Puerto Rico (No. 899). US Geological Survey.

1599   Moore, O.W., Buss, H.L., Green, S.M., Liu, M., & Song, Z. (2017). The importance of non-

1600   carbonate mineral weathering as a soil formation mechanism within a karst weathering profile in

1601   the SPECTRA Critical Zone Observatory, Guizhou Province, China. *Acta Geochim, 36*, 566–

1602   571. https://doi.org/10.1007/s11631-017-0237-4

1603   Moyes, H., Awe, J. J., Brook, G. A., & Webster, J. W. (2009). The ancient Maya drought cult:

1604   Late Classic cave use in Belize. *Latin American Antiquity*, *20*(1), 175-206.

1605   Musgrove, M., & Banner, J.L. (2004). Controls on the spatial and temporal variability of vadose

1606   dripwater geochemistry: Edwards aquifer, central Texas, *Geochimica et Cosmochimica Acta, 68,*

1607   1007–1020. https://doi.org/10.1016/j.gca.2003.08.014

1608   Mylroie, J.E., & Carew, J.L. (1990). The flank margin model for dissolution cave development

1609   in carbonate platforms. *Earth Surface Processes and Landforms, 15*, 413–424.

1610   National Research Council (2001). *Basic research opportunities in earth science.* National

1611   Academies Press.

1612   Newson, M. D. (1971). A model of subterranean limestone erosion in the British Isles based on

1613   hydrology. *Transactions of the Institute of British Geographers*, 55-70.

1614   Newton, J. G. (1987). *Development of sinkholes resulting from man's activities in the eastern*

1615   *United States* (Vol. 958). US Geological Survey.

1616   Noronha, A. L., Johnson, K. R., Southon, J. R., Hu, C., Ruan, J., & McCabe-Glynn, S. (2015).

1617   Radiocarbon evidence for decomposition of aged organic matter in the vadose zone as the main

1618   source of speleothem carbon. *Quaternary Science Reviews*, *127*, 37-47.

1619   Opdyke, N. D., Spangler, D. P., Smith, D. L., Jones, D. S., & Lindquist, R. C. (1984). Origin of

1620   the epeirogenic uplift of Pliocene-Pleistocene beach ridges in Florida and development of the

1621   Florida karst. *Geology*, *12*(4), 226-228.

1622 Oster, J. L., Covey, A. K., Lawrence, C. R., Giannetta, M. G., & Druhan, J. L. (2021). A reactive

1623 transport approach to modeling cave seepage water chemistry II: Elemental signatures.

1624 *Geochimica et Cosmochimica Acta*, 311, 353-373.

1625 Ott, R. F., Gallen, S. F., Caves Rugenstein, J. K., Ivy-Ochs, S., Helman, D., Fassoulas, C., et al.

1626 (2019). Chemical versus mechanical denudation in meta-clastic and carbonate bedrock

1627 catchments on Crete, Greece, and mechanisms for steep and high carbonate topography. *Journal*

1628 *of Geophysical Research: Earth Surface*, *124*(12), 2943-2961.

1629 Ott, R. F. (2020). How lithology impacts global topography, vegetation, and animal biodiversity:

1630 A global-scale analysis of mountainous regions. *Geophysical Research Letters, 47*(20),

1631 e2020GL088649.

1632 Palmer, A.N. (1991). Origin and morphology of limestone caves. *GSA Bulletin, 103*, 1–21.

1633 https://doi.org/10.1130/0016-7606(1991)103<0001:OAMOLC>2.3.CO;2

1634 Palmer, A.N. (2001). Dynamics of cave development by allogenic water. *Acta carsologica, 30,*

1635 13–32.

1636 Pané, F. R. (1999). An Account of the Antiquities of the Indians: A New Edition, with an

1637 Introductory Study, Notes, and Appendices by José Juan Arrom. Duke University Press.

1638 Panno, S. V., Kelly, W. R., Scott, J., Zheng, W., McNeish, R. E., Holm, N., ... & Baranski, E. L.

1639 (2019). Microplastic contamination in karst groundwater systems. *Groundwater*, *57*(2), 189-196.

1640 Parise, M., Ravbar, N., Živanović, V., Mikszewski, A., Kresic, N., Mádl-Szőnyi, J., & Kukurić,

1641 N. (2015). Hazards in karst and managing water resources quality. In *Karst aquifers—*

1642 *Characterization and engineering* (pp. 601-687). Springer, Cham.

1643 Patton, N.R., Lohse, K.A., Godsey, S.E., Crosby, B.T., & Seyfried, M.S. (2018). Predicting soil

1644 thickness on soil mantled hillslopes. *Nature Communications, 9*, 3329.

1645 https://doi.org/10.1038/s41467-018-05743-y

1646 Perrin, A. S., Probst, A., & Probst, J. L. (2008). Impact of nitrogenous fertilizers on carbonate

1647 dissolution in small agricultural catchments: Implications for weathering CO2 uptake at regional

1648 and global scales. *Geochimica et Cosmochimica Acta*, *72*(13), 3105-3123.

1649 Peterson, E.W., Wicks, C.M., 2005. Fluid and solute transport from a conduit to the matrix in a

1650 carbonate aquifer system. Mathematical Geology, 37, 851-867,

1651 Phillips, J.D., Pawlik, Ł., & Šamonil, P. (2019). Weathering fronts. *Earth-Science Reviews, 198*,

1652 102925. https://doi.org/10.1016/j.earscirev.2019.102925

1653 Pickering, R., Kramers, J. D., Hancox, P. J., de Ruiter, D. J., & Woodhead, J. D. (2011).

1654 Contemporary flowstone development links early hominin bearing cave deposits in South Africa.

1655 *Earth and planetary science letters*, *306*(1-2), 23-32.

1656 Plummer, L.N. (1975). Mixing of sea water with calcium carbonate ground water. *Geological*

1657 *Society of America Memoir, 142*, 219–236.

1658 Plummer, L. N., Wigley, T. M. L., & Parkhurst, D. L. (1978). The kinetics of calcite dissolution

1659 in CO 2-water systems at 5 degrees to 60 degrees C and 0.0 to 1.0 atm CO2. *American journal of*

1660 *science*, *278*(2), 179-216. https://doi.org/10.2475/ajs.278.2.179

1661 Plummer, L.N., Parkhurst, D.L., & Wigley, T.M.L. (1979). Critical review of the kinetics of

1662 calcite dissolution and precipitation. In *Chemical Modeling in Aqueous Systems.* ACS

1663 Publications, 537-573.

1664 Querejeta, J. I., Estrada-Medina, H., Allen, M. F., & Jiménez-Osornio, J. J. (2007). Water source

1665 partitioning among trees growing on shallow karst soils in a seasonally dry tropical climate.

1666 *Oecologia*, *152*, 26–36.

1667 Quine, T., Guo, D., Green, S. M., Tu, C., Hartley, I., Zhang, X., ... & Meersmans, J. (2017).

1668 Ecosystem service delivery in Karst landscapes: anthropogenic perturbation and recovery. *Acta*

1669 *Geochimica*, 36(3), 416-420.

1670   Quinlan, J. F., Davies, G. J., Jones, S. W., & Huntoon, P. W. (1996). The applicability of

1671   numerical models to adequately characterize ground-water flow in karstic and other triple-

1672   porosity aquifers. *Subsurface fluid-flow (ground-water and vadose zone) modeling, ASTM STP*,

1673   *1288*, 114-133.

1674   Reich, P. B., & Borchert, R. (1984). Water stress and tree phenology in a tropical dry forest in

1675   the lowlands of Costa Rica. *Journal of Ecology, 72*, 61-74.

1676   Rempe, D.M., & Dietrich, W.E. (2014). A bottom-up control on fresh-bedrock topography under

1677   landscapes. *Proceedings of the National Academy of Sciences, 111*, 6576–6581.

1678   https://doi.org/10.1073/pnas.1404763111

1679   Riebe, C. S., Kirchner, J. W., Granger, D. E., & Finkel, R. C. (2001). Strong tectonic and weak

1680   climatic control of long-term chemical weathering rates. *Geology*, *29*(6), 511-514.

1681   Riebe, C.S., Hahm, W.J., & Brantley, S.L. (2017). Controls on deep critical zone architecture: a

1682   historical review and four testable hypotheses. *Earth Surface Processes and Landforms, 42*, 128–

1683   156. https://doi.org/10.1002/esp.4052

1684   Roland, M., Serrano-Ortiz, P., Kowalski, A. S., Goddéris, Y., Sánchez-Cañete, E. P., Ciais, P., ...

1685   & Janssens, I. A. (2013). Atmospheric turbulence triggers pronounced diel pattern in karst

1686   carbonate geochemistry. Biogeosciences, 10(7), 5009-5017.

1687   Romero-Mujalli, G., Hartmann, J., Börker, J., Gaillardet, J., & Calmels, D. (2019). Ecosystem

1688   controlled soil-rock pCO2 and carbonate weathering – Constraints by temperature and soil water

1689   content. *Chemical Geology, 527*, 118634. https://doi.org/10.1016/j.chemgeo.2018.01.030

1690   Rossinsky, V., & Wanless, H. R. (1992). Topographic and vegetative controls on calcrete

1691   formation, Turks and Caicos Islands, British West Indies. *Journal of Sedimentary Research*,

1692   *62*(1), 84-98.

1693   Ryb, U., Matmon, A., Erel, Y., Haviv, I., Katz, A., Starinsky, A., et al. (2014). Controls on

1694   denudation rates in tectonically stable Mediterranean carbonate terrain. *Geological Society of*

1695   *America Bulletin, 126,* 553–568. https://doi.org/10.1130/B30886.1

1696   Sanchez-Cañete, E. P., Serrano-Ortiz, P., Kowalski, A. S., Oyonarte, C., & Domingo, F. (2011).

1697   Subterranean CO2 ventilation and its role in the net ecosystem carbon balance of a karstic

1698   shrubland. *Geophysical research letters*, *38*(9). https://doi.org/10.1029/2011GL047077

1699   Schulze-Makuch, D., Carlson, D. A., Cherkauer, D. S., & Malik, P. (1999). Scale dependency of

1700   hydraulic conductivity in heterogeneous media. *Ground Water, 37*(8), 904-919.

1701   Scribner, C. A., Martin, E. E., Martin, J. B., Deuerling, K. M., Collazo, D. F., & Marshall, A. T.

1702   (2015). Exposure age and climate controls on weathering in deglaciated watersheds of western

1703   Greenland. *Geochimica et Cosmochimica Acta*, *170*, 157-172.

1704   Sekhon, N., Novello, V. F., Cruz, F. W., Wortham, B. E., Ribeiro, T. G., & Breecker, D. O.

1705   (2021). Diurnal to seasonal ventilation in Brazilian caves. Global and Planetary Change, 197,

1706   103378.

1707   Shaughnessy, A. R., Gu, X., Wen, T., & Brantley, S. L. (2021). Machine learning deciphers

1708   CO2 sequestration and subsurface flowpaths from stream chemistry. *Hydrology and*

1709   *Earth System Sciences, 25*(6), 3397-3409.

1710   Siemers, J., & Dreybrodt, W. (1998). Early development of Karst aquifers on percolation

1711   networks of fractures in limestone. *Water Resour. Res., 34*, 409–419.

1712   https://doi.org/10.1029/97WR03218

1713   Simms, M.J. (2004). Tortoises and hares: dissolution, erosion and isostasy in landscape

1714   evolution. *Earth Surf. Process. Landforms, 29,* 477–494. https://doi.org/10.1002/esp.1047

1715   Smith, D.I., & Atkinson, T.C. (1976). Process, Landforms and Climate in Limestone Regions.

1716   *Geomorphology and climate, 512.*

1717   Smart, P., Waltham, T., Yang, M., & Zhang, Y. J. (1986). Karst geomorphology of western

1718   Guizhou, China. *Cave Science*, *13*(3).

1719   Spalding, R. F., & Mathews, T. D. (1972). Stalagmites from caves in the Bahamas: Indicators of

1720   low sea level stand. *Quaternary Research*, 2(4), 470-472.

1721   Spellman, P., Gulley, J., Martin, J. B., & Loucks, J. (2019). The role of antecedent groundwater

1722   heads in controlling transient aquifer storage and flood peak attenuation in karst watersheds.

1723   *Earth Surface Processes and Landforms*, *44*(1), 77-87.

1724   Spötl, C., Fairchild, I. J., & Tooth, A. F. (2005). Cave air control on dripwater geochemistry,

1725   Obir Caves (Austria): Implications for speleothem deposition in dynamically ventilated caves.

1726   *Geochimica et Cosmochimica Acta*, *69*(10), 2451-2468.

1727   https://doi.org/10.1016/j.gca.2004.12.009

1728   Stevanović, Z. (2018). Global distribution and use of water from karst aquifers. *Geological*

1729   *Society, London, Special Publications*, *466*(1), 217-236.

1730   Stock, G.M., Granger, D.E., Sasowsky, I.D., Anderson, R.S., & Finkel, R.C. (2005). Comparison

1731   of U–Th, paleomagnetism, and cosmogenic burial methods for dating caves: implications for

1732   landscape evolution studies. *Earth and Planetary Science Letters, 236*(1-2), 388-403.

1733   Stoll, H. M., Müller, W., & Prieto, M. (2012). I-STAL, a model for interpretation of Mg/Ca,

1734   Sr/Ca and Ba/Ca variations in speleothems and its forward and inverse application on seasonal to

1735   millennial scales. *Geochemistry, Geophysics, Geosystems*, *13*(9).

1736   Stoll, H. M., Cacho, I., Gasson, E., Sliwinski, J., Kost, O., Moreno, A., ... & Edwards, R. L.

1737   (2022). Rapid northern hemisphere ice sheet melting during the penultimate deglaciation. *Nature*

1738   *communications*, *13*(1), 1-16.

1739   Ström, L., Owen, A. G., Godbold, D. L., & Jones, D. L. (2005). Organic acid behaviour in a

1740   calcareous soil implications for rhizosphere nutrient cycling. *Soil Biology & Biochemistry, 37*,

1741   2046–2054.

1742   Sullivan, P.L., Stops, M.W., Macpherson, G.L., Li, L., Hirmas, D.R., & Dodds, W.K. (2019).

1743   How landscape heterogeneity governs stream water concentration-discharge behavior in

1744   carbonate terrains (Konza Prairie, USA). *Chemical Geology, 527*, 118989.

1745   https://doi.org/10.1016/j.chemgeo.2018.12.002

1746   Sullivan, P.L., Wymore, A.S., McDowell, M., Aarons, S., Aciego, S., Anders, A.M., et al.

1747   (2017). New opportunities for Critical Zone science, In: *2017 CZO Arlington Meeting White*

1748   *Booklet*.

1749   Sullivan, P. L., Zhang, C., Behm, M., Zhang, F., & Macpherson, G. L. (2020). Toward a new

1750   conceptual model for groundwater flow in merokarst systems: Insights from multiple

1751   geophysical approaches. *Hydrological Processes*, *34*(24), 4697-4711.

1752   Surić, M., Richards, D. A., Hoffmann, D. L., Tibljaš, D., & Juračić, M. (2009). Sea-level change

1753   during MIS 5a based on submerged speleothems from the eastern Adriatic Sea (Croatia). *Marine*

1754   *Geology*, 262(1-4), 62-67.

1755   Sutikna, T., Tocheri, M. W., Morwood, M. J., Saptomo, E. W., Awe, R. D., Wasisto, S., ... &

1756   Roberts, R. G. (2016). Revised stratigraphy and chronology for Homo floresiensis at Liang Bua

1757   in Indonesia. *Nature*, *532*(7599), 366-369.

1758   Svensson, U., & Dreybrodt, W. (1992). Dissolution kinetics of natural calcite minerals in CO2-

1759   water systems approaching calcite equilibrium. *Chemical Geology, 100*, 129–145.

1760   Swaffer, B. A., Holland, K. L., Doody, T. M., Li, C., & Hutson, J. (2014). Water use strategies of

1761   two co-occurring tree species in a semi-arid karst environment. *Hydrological Processes, 28*,

1762   2003–2017.

1763   Szymczak, P., & Ladd, A.J.C. (2011). The initial stages of cave formation: Beyond the one-

1764   dimensional paradigm. *Earth and Planetary Science Letters, 301*, 424–432.

1765   Szymczak, P., & Ladd, A.J.C. (2012). Reactive-infiltration instabilities in rocks. Fracture

1766   dissolution. *J. Fluid Mech., 702*, 239–264. https://doi.org/10.1017/jfm.2012.174

1767   https://doi.org/10.1016/j.epsl.2010.10.026

1768   Tennyson, R., Brahana, V., Polyak, V.J., Potra, A., Covington, M., Asmerom, Y., et al. (2017).

1769   Hypogene Speleogenesis in the Southern Ozark Uplands, Mid-Continental United States, In:

1770   Klimchouk, A. N., Palmer, A., De Waele, J., S. Auler, A., & Audra, P. (Eds.), Hypogene Karst

1771   Regions and Caves of the World. Springer International Publishing, Cham, pp. 663–676.

1772   https://doi.org/10.1007/978-3-319-53348-3_43

1773   Tobin, B. W., Polk, J. S., Arpin, S. M., Shelley, A., & Taylor, C. (2021). A conceptual model of

1774   epikarst processes across sites, seasons, and storm events. *Journal of Hydrology*, 596, 125692.

1775   Tooth, A.F., & Fairchild, I.J. (2003). Soil and karst aquifer hydrological controls on the

1776   geochemical evolution of speleothem-forming drip waters, Crag Cave, southwest Ireland.

1777   *Journal of Hydrology, 273*, 51–68. https://doi.org/10.1016/S0022-1694(02)00349-9

1778   Torres, M. A., A. J. West, & Li, G. (2014). Sulphide oxidation and carbonate dissolution as a

1779   source of CO2 over geological timescales, *Nature, 507*(7492), 346-349.

1780   Treble, P. C., Baker, A., Abram, N. J., Hellstrom, J. C., Crawford, J., Gagan, M. K., ... &

1781   Paterson, D. (2022). Ubiquitous karst hydrological control on speleothem oxygen isotope

1782   variability in a global study. *Communications Earth & Environment*, *3*(1), 1-10.

1783   Troester, J. W., White, E. L., & White, W. B. (1984). A comparison of sinkhole depth frequency

1784   distributions in temperate and tropic karst regions. In *Multidisciplinary conference on sinkholes.*

1785   *1* (pp. 65-73).

1786   Vacher, H.L., & Mylroie, J.E. (2002). Eogenetic karst from the perspective of an equivalent

1787   porous medium. *Carbonates and Evaporites*, *17*, 182.

1788   Veni, G., DuChene, H., & Groves, C. (2001). Living with Karst: A Fragile

1789   Foundation—American Geological Institute Environmental Awareness Series 4. *American*

1790   *Geological Institute, Alexandria*, 7.

1791   Vesper, D. J., & White, W. B. (2003). Metal transport to karst springs during storm flow: an

1792   example from Fort Campbell, Kentucky/Tennessee, USA. *Journal of Hydrology*, *276*(1-4), 20-

1793   36.

1794   Vesper, D. J., & White, W. B. (2004). Storm pulse chemographs of saturation index and carbon

1795   dioxide pressure: implications for shifting recharge sources during storm events in the karst

1796   aquifer at Fort Campbell, Kentucky/Tennessee, USA. *Hydrogeology Journal*, *12*(2), 135-143.

1797   https://doi.org/10.1007/s10040-003-0299-8

1798   Wagner, T., Fritz, H., Stüwe, K., Nestroy, O., Rodnight, H., Hellstrom, J., et al. 2(011).

1799   Correlations of cave levels, stream terraces and planation surfaces along the River Mur—Timing

1800   of landscape evolution along the eastern margin of the Alps. *Geomorphology*, *134*, 62–78.

1801   https://doi.org/10.1016/j.geomorph.2011.04.024

1802   Waltham, T. (2008). Sinkhole hazard case histories in karst terrains. *Quarterly Journal of*

1803   *Engineering Geology and Hydrogeology*, *41*(3), 291-300.

1804   Wen, H., Sullivan, P. L., Macpherson, G. L., Billings, S. A., & Li, L. (2021). Deepening roots

1805   can enhance carbonate weathering by amplifying CO 2-rich recharge. *Biogeosciences*, *18*(1), 55-

1806   75.

1807   West, A. J., Galy, A., & Bickle, M. (2005). Tectonic and climatic controls on silicate weathering.

1808   *Earth and Planetary Science Letters*, *235*(1-2), 211-228.

1809   White, W.B. (2002). Karst hydrology: recent developments and open questions. *Engineering*

1810   *Geology, 65*, 85–105. https://doi.org/10.1016/S0013-7952(01)00116-8

1811   White, W.B. (1984). Rate processes: chemical kinetics and karst landform development. In

1812   *Groundwater as a Geomorphic Agent*. Routledge: London.

1813   https://doi.org/10.4324/9781003028833

1814   White, W.B., Herman, E., Rutigliano, M., Herman, J., Vesper, D., & Engel, S. (2016). Karst

1815   groundwater contamination and public health. *Karst Waters Inst. Spec. Publ. 19*, Springer.

1816   White, W.B., & White, E.L. (2005). Size scales for closed depression landforms: The place of

1817   tiankengs. *Cave and Karst Science, 32*(2/3), 111.

1818   Wigley, T.M.L., & Plummer, L.N. (1976). Mixing of carbonate waters. *Geochimica et*

1819   *Cosmochimica Acta, 40*, 989–995. https://doi.org/10.1016/0016-7037(76)90041-7

1820   Williams, P. (2008a). The role of the epikarst in karst and cave hydrogeology: a review.

1821   *International Journal of Speleology, 37*. http://dx.doi.org/10.5038/1827-806X.37.1.1

1822   Williams, P. (2008b). *World Heritage Caves and Karst: A thematic study*. Gland, Switzerland:

1823   IUCN 57pp.

1824   Williams, P.W. (1985). Subcutaneous hydrology and the development of doline and cockpit

1825   karst. *Zeitschrift für Geomorphologie, 29*, 463–482.

1826   Wilson, D. J., Von Strandmann, P. A. P., White, J., Tarbuck, G., Marca, A. D., Atkinson, T. C.,

1827   & Hopley, P. J. (2021). Seasonal variability in silicate weathering signatures recorded by Li

1828   isotopes in cave drip-waters. *Geochimica et Cosmochimica Acta*, 312, 194-216.

1829   Wolfe, B. T., & Kursar, T. A. (2015). Diverse patterns of stored water use among saplings in

1830   seasonally dry tropical forests. *Oecologia, 179*, 925–936.

1831   Wong, C.I., Banner, J.L., & Musgrove, M. (2011). Seasonal dripwater Mg/Ca and Sr/Ca

1832   variations driven by cave ventilation: Implications for and modeling of speleothem paleoclimate

1833   records. *Geochimica et Cosmochimica Acta, 75*, 3514–3529.

1834   https://doi.org/10.1016/j.gca.2011.03.025

1835   Wood, W.W. (1985). Origin of caves and other solution openings in the unsaturated (vadose)

1836   zone of carbonate rocks: A model for CO2 generation. *Geology*, *13*, 822–824.

1837   Wood, W.W., & Petraitis, M.J. (1984). Origin and Distribution of Carbon Dioxide in the

1838   Unsaturated Zone of the Southern High Plains of Texas. *Water Resour. Res., 20*, 1193–1208.

1839   https://doi.org/10.1029/WR020i009p01193

1840   Worthington, S.R. (1999). A comprehensive strategy for understanding flow in carbonate

1841   aquifers, in: *Karst Modeling, Karst Waters Institute Special Publication 5. Karst Waters*

1842   *Institute*, pp. 30–37.

1843   Worthington, S.R.H. (2009). Diagnostic hydrogeologic characteristics of a karst aquifer

1844   (Kentucky, USA). *Hydrogeol J, 17*, 1665–1678. https://doi.org/10.1007/s10040-009-0489-0

1845   Worthington, S.R.H., Davies, G.J., & Alexander, E.C. (2016). Enhancement of bedrock

1846   permeability by weathering. *Earth-Science Reviews*, *160*, 188–202.

1847   https://doi.org/10.1016/j.earscirev.2016.07.002

1848   Wray, R.A.L., & Sauro, F. (2017). An updated global review of solutional weathering processes

1849   and forms in quartz sandstones and quartzites. *Earth-Science Reviews, 171*, 520–557.

1850   https://doi.org/10.1016/j.earscirev.2017.06.008

1851   Yizhaq, H., Ish-Shalom, C., Raz, E., & Ashkenazy, Y. (2017). Scale-free distribution of Dead

1852   Sea sinkholes: Observations and modeling. *Geophysical Research Letters*, *44*(10), 4944-4952.

1853   Zanolli, C., Davies, T. W., Joannes-Boyau, R., Beaudet, A., Bruxelles, L., de Beer, F., ... &

1854   Skinner, M. M. (2022). Dental data challenge the ubiquitous presence of Homo in the Cradle of

1855   Humankind. *Proceedings of the National Academy of Sciences*, *119*(28), e2111212119.

1856 Zeng, Q., Liu, Z., Chen, B., Hu, Y., Zeng, S., Zeng, C., et al. (2017). Carbonate weathering-

1857 related carbon sink fluxes under different land uses: A case study from the Shawan Simulation

1858 Test Site, Puding, Southwest China. *Chemical Geology, 474*, 58–71.

1859 Zhao, L., & Hou, R. (2019). Human causes of soil loss in rural karst environments: a case study

1860 of Guizhou, China. *Scientific Reports*, *9*(1), 1-11. doi:10.1038/s41598-018-35808-3

1861 Zhao, S., Pereira, P., Wu, X., Zhou, J., Cao, J., & Zhang, W. (2020). Global karst vegetation

1862 regime and its response to climate change and human activities. *Ecological Indicators*, *113*,

1863 106208.

1864 Zorn, M., Erhartic, B., Komac, B., & Gauchon, C. (2009). La Slovénie, berceau du géotourisme

1865 karstique. *Karstologia*, *54*(1), 1–10. https://doi.org/10.3406/karst.2009.2655